

The transcriptional landscape of $\alpha\beta$ T cell differentiation

Michael Mingueneau^{1,9}, Taras Kreslavsky^{2,9}, Daniel Gray^{3,4,9}, Tracy Heng^{5,9}, Richard Cruse¹, Jeffrey Ericson¹, Sean Bendall⁶, Matthew H Spitzer⁶, Garry P Nolan⁶, Koichi Kobayashi^{2,7}, Harald von Boehmer², Diane Mathis¹, Christophe Benoist¹ & the Immunological Genome Consortium⁸

The differentiation of $\alpha\beta$ T cells from thymic precursors is a complex process essential for adaptive immunity. Here we exploited the breadth of expression data sets from the Immunological Genome Project to analyze how the differentiation of thymic precursors gives rise to mature T cell transcriptomes. We found that early T cell commitment was driven by unexpectedly gradual changes. In contrast, transit through the CD4⁺CD8⁺ stage involved a global shutdown of housekeeping genes that is rare among cells of the immune system and correlated tightly with expression of the transcription factor c-Myc. Selection driven by major histocompatibility complex (MHC) molecules promoted a large-scale transcriptional reactivation. We identified distinct signatures that marked cells destined for positive selection versus apoptotic deletion. Differences in the expression of unexpectedly few genes accompanied commitment to the CD4⁺ or CD8⁺ lineage, a similarity that carried through to peripheral T cells and their activation, demonstrated by mass cytometry phosphoproteomics. The transcripts newly identified as encoding candidate mediators of key transitions help define the 'known unknowns' of thymocyte differentiation.

The Immunological Genome Project (ImmGen) is an international collaboration of laboratories that collectively perform a thorough dissection of gene expression and its regulation in the immune system of the mouse. Here we tracked the transcriptome through the entire differentiation pathway of T cells in the thymus against the backdrop of all ImmGen data. Through this analysis, we identified unexpectedly gradual changes, sharp breakpoints and unanticipated similarities.

Hematopoietic precursors differentiate into T cells in the vertebrate thymus. This differentiation process has been studied intensively over several decades¹, which has resulted in what is arguably the most finely parsed of any differentiation cascade among mammalian cell types^{2–9}. The sequence runs from the commitment of lymphoid precursors to the T cell lineage, to the random rearrangement of genes encoding T cell antigen receptors (TCRs) and their subsequent selection that allows maturation of only those thymocytes bearing potentially useful TCR specificities (positive selection) and that do not overreact to self (negative selection). These steps are distinguished by the expression of certain cell-surface molecules. The most immature thymocytes lack expression of the coreceptors CD4 and CD8 (and are thus CD4[–]CD8[–] double-negative (DN) cells) and can be further subcategorized into subsets that track the commitment to becoming T cells with expression of the markers CD25, CD44 (ref. 10), c-Kit¹¹ and CD28 (ref. 12). Functional rearrangement and expression of a $\gamma\delta$ TCR promotes proliferation accompanied by early maturation of DN progenitors and subsequent emigration from the thymus¹³.

In contrast, successful rearrangement of the gene encoding TCR β in the DN subset initiates several rounds of proliferation essential for $\alpha\beta$ differentiation and the generation of CD4⁺CD8⁺ double-positive (DP) thymocytes¹⁴, in which TCR α rearrangement takes place. DP thymocytes screen thymic cortical epithelial cells for the potential of their TCR to interact with complexes of peptide and major histocompatibility complex (MHC)^{15–18}. Those DP thymocytes bearing TCRs that cannot bind self peptide–MHC (thought to be the majority) die within 3–4 d (ref. 19). Those DP thymocytes that express a TCR that can interact with MHC class I or MHC class II molecules are positively selected and correspondingly mature as CD4[–]CD8⁺ single-positive (CD8SP) or CD4⁺CD8[–] single-positive (CD4SP) thymocytes (lineage commitment)²⁰. This positive selection process differs from β -selection, as it occurs in absence of extensive proliferation. If the affinity of the TCR-peptide–MHC interaction is too high, thymocytes are eliminated by apoptosis (clonal deletion) or are diverted into alternative lineages such as CD8 $\alpha\alpha$ ⁺ T cells or Foxp3⁺ regulatory T cells^{21,22}. Thymocytes that survive these processes are exported from the thymus and undergo a phase of post-thymic maturation to become functional CD4⁺ or CD8⁺ T cells²³.

Several of the molecular mediators required for progression through certain stages of thymocyte differentiation have been defined by genetic approaches. What is lacking is a general perspective of how those and other pathways integrate to direct thymocyte differentiation in an unperturbed system. Although many studies have profiled thymocyte transcriptomes^{24–33}, they focused on only limited transitions

¹Division of Immunology, Department of Microbiology and Immunobiology, Harvard Medical School, Boston, Massachusetts, USA. ²Dana-Farber Cancer Institute, Boston, Massachusetts, USA. ³Department of Medical Biology, University of Melbourne, Parkville, Australia. ⁴Molecular Genetics of Cancer Division and Immunology Division, The Walter and Eliza Hall Institute of Medical Research, Parkville, Victoria, Australia. ⁵Department of Anatomy and Developmental Biology, Monash University, Clayton, Victoria, Australia. ⁶Department of Microbiology and Immunology, Stanford University School of Medicine, Palo Alto, California, USA. ⁷Department of Microbial and Molecular Pathogenesis, Texas A&M Health Science Center, College Station, Texas, USA. ⁸A full list of members and affiliations appears at the end of the paper. ⁹These authors contributed equally to this work. Correspondence should be addressed to C.B. (cbdm@hms.harvard.edu) or D.M. (cbdm@hms.harvard.edu).

Received 30 November 2012; accepted 19 March 2013; published online 5 May 2013; corrected online 13 May 2013 (details online); doi:10.1038/ni.2590

or selected checkpoints. Here we revisited the entire spectrum of differentiation states in the $\alpha\beta$ T cell branch of the lymphoid tree from a transcriptional standpoint, using the breadth of ImmGen data sets. This analysis showed unexpected aspects of T cell differentiation and identified candidate genes whose coordinated regulation at certain transitions hinted at important functions during thymocyte selection and maturation.

RESULTS

Overall perspective of T cell differentiation

We generated gene-expression profiles from every stage of thymocyte maturation, from early thymic progenitor (ETP) to the most mature SP thymocyte ready for export from the thymus (complete list of population names, abbreviations and markers used for cell sorting, **Supplementary Table 1**). We also included profiles from bone marrow progenitors and peripheral naive T cells. All data sets were generated in duplicate or triplicate from cells obtained from 6-week-old C57Bl/6 male mice. To validate these data, we first assessed the activity of over 50 well-characterized genes that mark key events in thymocyte differentiation, such as *Rag1*, *Tcr α* and *Tcr β* , and observed the expected expression patterns (**Fig. 1a**, **Supplementary Fig. 1** and data not shown). We used several mathematical tools for multivariate analysis to determine the relationships between populations. Unsupervised hierarchical clustering reproduced the known differentiation sequence with notable accuracy (**Fig. 1b**), which indicated that there were no hidden, unexpected findings in the $\alpha\beta$ T cell branch of the hematopoietic tree determined over the past three decades and that transcriptional relationships do evolve linearly along differentiation.

We then used principal-component analysis to map cell populations in three-dimensional space (**Fig. 1c**), which again matched the differentiation sequence but also grouped stages into distinct 'pods', such as the tightly knit group of mature SP cells. Principal-component analysis of the entire ImmGen data set identified a dominant component (PC1; 73% of variance) that tracked 'generically' with maturation in lineages of the immune system (data not shown), reminiscent of the major 'differentiation' component observed in multivariate mass cytometry analysis of bone marrow cells³⁴. The maturation of $\gamma\delta$ T cells proceeded directly from precursors at DN stage 3 (DN3), whereas $\alpha\beta$ T cells first 'regressed' along this principal component through the intermediate SP (ISP) and DP stages. For subsequent analyses, we excluded $\gamma\delta$ T cells³⁵ and the DN4 subset (which incorporates both $\alpha\beta$ TCR and $\gamma\delta$ TCR thymocytes).

We visualized the magnitude of transcriptional changes throughout differentiation better by plotting the cumulative Euclidean distance between populations (**Fig. 1d**) and the number of transcripts induced or repressed at each transition (**Fig. 1e**). These two metrics identified three main 'tectonic shifts': between bone marrow precursors and ETPs; at the transition through DN3a; and (the strongest such shift) around the DP compartment. Contrary to what has been shown for cells that develop when cultured with OP9 mouse bone marrow stromal cells expressing the Notch ligand Delta-like 1 (OP9-DL1 cells)³¹, *in vivo* commitment to the T cell lineage at the DN2a-to-DN2b transition was associated with relatively moderate changes (**Fig. 1d,e**). Although DP blasts resembled earlier β -selected populations, small DP cells were very different. Small DP thymocytes were also very different from CD69⁺ DP thymocytes, which indicated that TCR signaling in DP thymocytes initiated yet another major transcriptional change. In contrast, the transition from CD69⁺ DP thymocyte to terminal CD4SP or CD8SP cell involved comparatively minor changes, and CD4⁺ or CD8⁺ cells looked extremely similar from this perspective (**Fig. 1d,e**). Finally, egress from the thymus to

the periphery had a very small effect on transcription. Thus, relationships among the transcriptomes recapitulated the accepted developmental progression of thymocyte differentiation and provided several new insights into the transcriptional basis of key transitions.

Early T cell differentiation

The major landmarks of early T cell differentiation (that is, loss of B cell potential at the ETP stage and irreversible commitment to the T cell lineage at the DN2a-to-DN2b transition) happen in a rather discrete manner⁹. In contrast, the transcriptional changes in most genes, including those encoding many key regulators, were gradual. For example, the expression of *Bcl11b*, which encodes a T lineage-commitment factor^{32,36,37}, not only increased from the DN2a stage to the DN2b stage, when commitment actually occurs, but also before (ETP to DN2a) and after (DN2b to DN3a) that time (**Supplementary Fig. 1**). The gradual nature of gene expression changes was a common feature throughout early T cell differentiation (discussed below) and may indicate that these transitions are not 'radical' events but instead proceed by degrees or, more prosaically, that they are not synchronized with changes in the few cell-surface markers used to identify differentiation intermediates.

To group those transcripts with similar behavior during early thymocyte differentiation, we applied k-means clustering to the set of 2,088 genes with the most variable expression. The resulting clusters (named by a characteristic gene or group of genes; **Fig. 2a,b** and **Supplementary Table 2**) included not only genes encoding molecules with previously assigned functions in thymocyte differentiation (for example, about half of the probes for the '*Tcf-1* and *Lef-1*' and '*Cd4* and *Cd8*' clusters) but also many genes whose functions have not yet been studied in T cells to our knowledge, which provided a rich resource for discovering additional molecular participants in thymocyte differentiation.

An important feature of early T cell differentiation is the shutdown of programs of progenitor and non-T cell lineages³⁸. The '*c-Kit*', '*Cd34*' and 'PU.1' clusters (**Fig. 2a,b** and **Supplementary Table 2**) contained genes that were gradually downregulated from hematopoietic stem cells to DN3 cells, including those encoding markers of hematopoietic progenitor cells, such as *Flt3*, *Cd34*, *Ly6a* (Sca-1) and *Kit*, as well as a small group of genes typical of non-T cell lineages (B cells, NK cells or myeloid cells). Transcriptional regulators in these clusters included those encoded by *Bcl11a*, *Hhex*, *Jun*, *Meis1*, *Mef2c* and *Sfp1* (PU.1) (**Fig. 2c**).

Commitment to the T cell lineage is associated with the rearrangement of *Tcrb*, *Tcr α* and *Tcrd* loci and induction of TCR signaling machinery. The '*Gata-3*' and '*Tcf-1* and *Lef-1*' clusters that were upregulated in early thymocytes and reached a plateau around the DN3a stage of T cell differentiation (**Fig. 2a,b**) included genes encoding molecules involved in recombination (*Rag1* and *Lig4*) and a major subset of genes encoding molecules related to TCR signaling (*Cd3d*, *Cd3e*, *Cd3g*, *Lck*, *Itk*, *Grp2* (GADS), *Rasgrp1*, *Zap70*, *Cbl* and *Nck2*; **Supplementary Fig. 2**). Several notable genes encoding proteins with probable signaling functions were also in these clusters (**Fig. 2b**). For example, *Arpp21* encodes RCS, which is a competitive inhibitor of calmodulin-dependent enzymes, including calcineurin³⁹, and is thus a putative negative regulator of TCR signaling. A thymocyte-specific isoform of this protein is reported to be expressed from DN2 onward and downregulated after positive selection⁴⁰. The diacylglycerol (DAG) kinase DGK ϵ (encoded by *Dgke*), which converts DAG to phosphatidic acid, may also regulate TCR signaling at this stage, as has been suggested for DGK- α and DGK- ζ ^{41,42}. More generally, there were notable shifts in the entire DGK family during thymocyte differentiation (**Fig. 2d**).

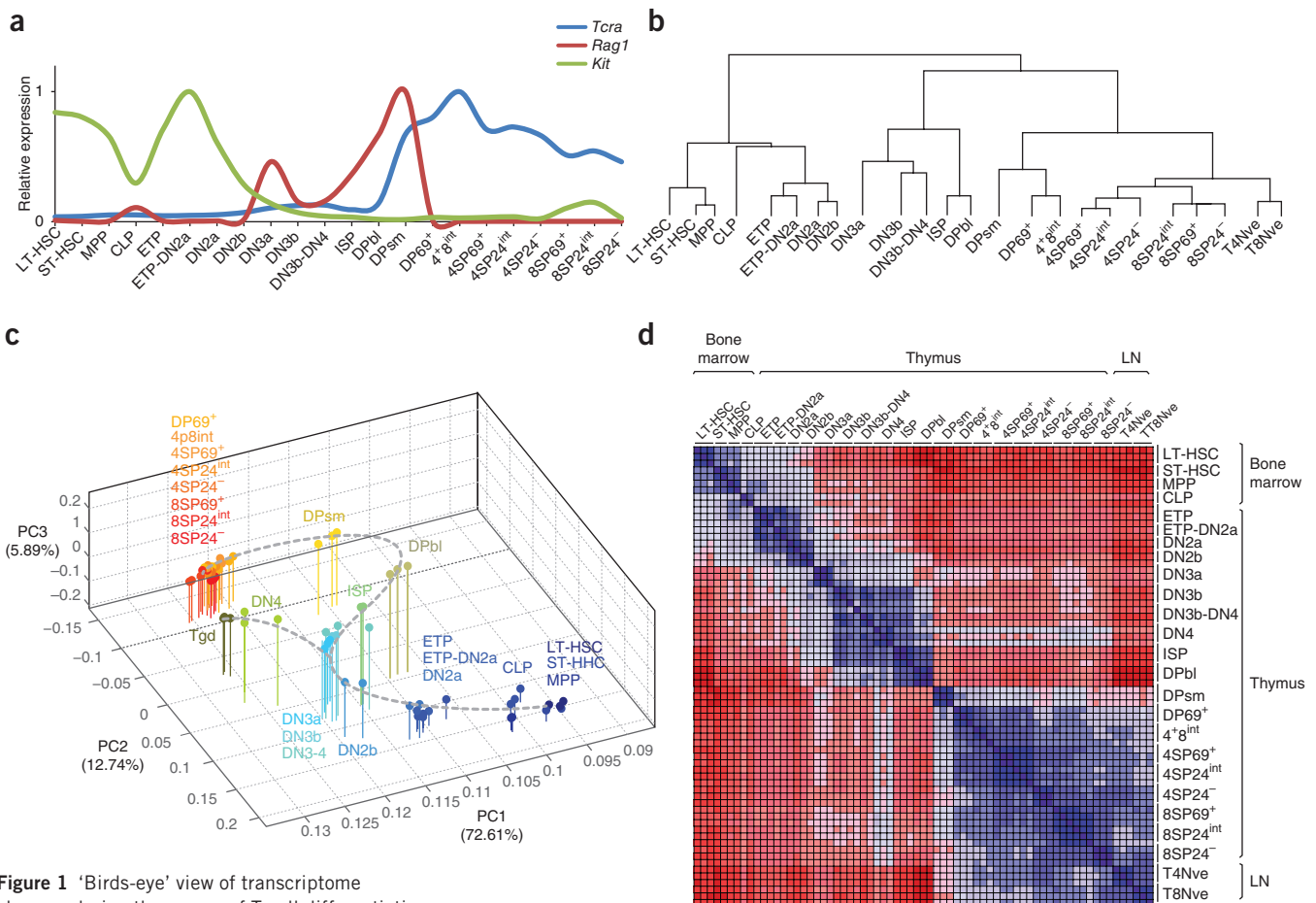


Figure 1 'Birds-eye' view of transcriptome changes during the course of T cell differentiation.

(a) Expression of *Tcr*, *Rag1* and *Kit* in various bone marrow and thymocyte populations (horizontal axis; abbreviations, **Supplementary Table 1**), presented as the maximum-normalized mean. (b–d) Hierarchical clustering (b), principal-component analysis (c) and heat map of Euclidian distances between various populations (d; top and right margins), calculated with the 15% of probes with the greatest difference in expression among these subsets and with expression values >120 for at least one of the subsets. Expression values were log²-transformed and row-standardized before the analysis. (e) Probes upregulated (red) or downregulated (blue) by twofold or more at various transitions (arrows, horizontal axis) during T cell differentiation. Filled symbols, total probes; open symbols, probes not part of the proliferation signature.

Signaling via the Notch family of receptors is necessary for commitment to the T cell lineage and is indispensable at all steps of T cell differentiation before the DP stage^{8,9}. Direct Notch targets were distributed across multiple clusters with very different patterns of expression. Many canonical Notch targets, such as *Ptcr*a (which encodes pre-TCR α)^{43,44}, *Dtx1*, *Il7r*⁴⁵ and *Notch1* itself⁴⁶ were in the 'preTCR α ' and 'Il7r' clusters that peaked around DN3a (Fig. 2a), consistent with the idea that DN3a cells receive the strongest Notch signaling^{46,47}. A few targets, such as *Nrarp* and *Hes1* (in corresponding clusters), were upregulated and reached a plateau as early as in ETP thymocytes (Fig. 2a). Two Notch targets of particular interest were the transcription factor-encoding genes *Tcf7* (refs. 48,49) and *Bcl11b*^{32,36,37} (both in the 'Tcf-1 and Lef-1' cluster). These genes were upregulated early, then their expression reached a plateau by DN3a and was maintained

high thereafter, even after downmodulation of Notch signaling after β -selection. Thus, Notch signaling is required for the induction but not the maintenance of these key regulators of T cell differentiation, consistent with the finding that Notch is required early in T cell differentiation but is dispensable for maintenance of T cell identity. Finally, *Myc*⁵⁰ (from the '*c-Myc*' cluster) had yet another pattern of steady expression early and an abrupt decrease in expression in DP thymocytes. It is therefore very likely that additional factors other than Notch regulate expression of Notch targets, which results in the observed diversity of expression patterns in early thymocyte differentiation.

T cell program induced by β -selection

TCR β proteins formed after productive rearrangements of the *Tcrb* locus combine with the germline-encoded pre-TCR α chain (preTCR)



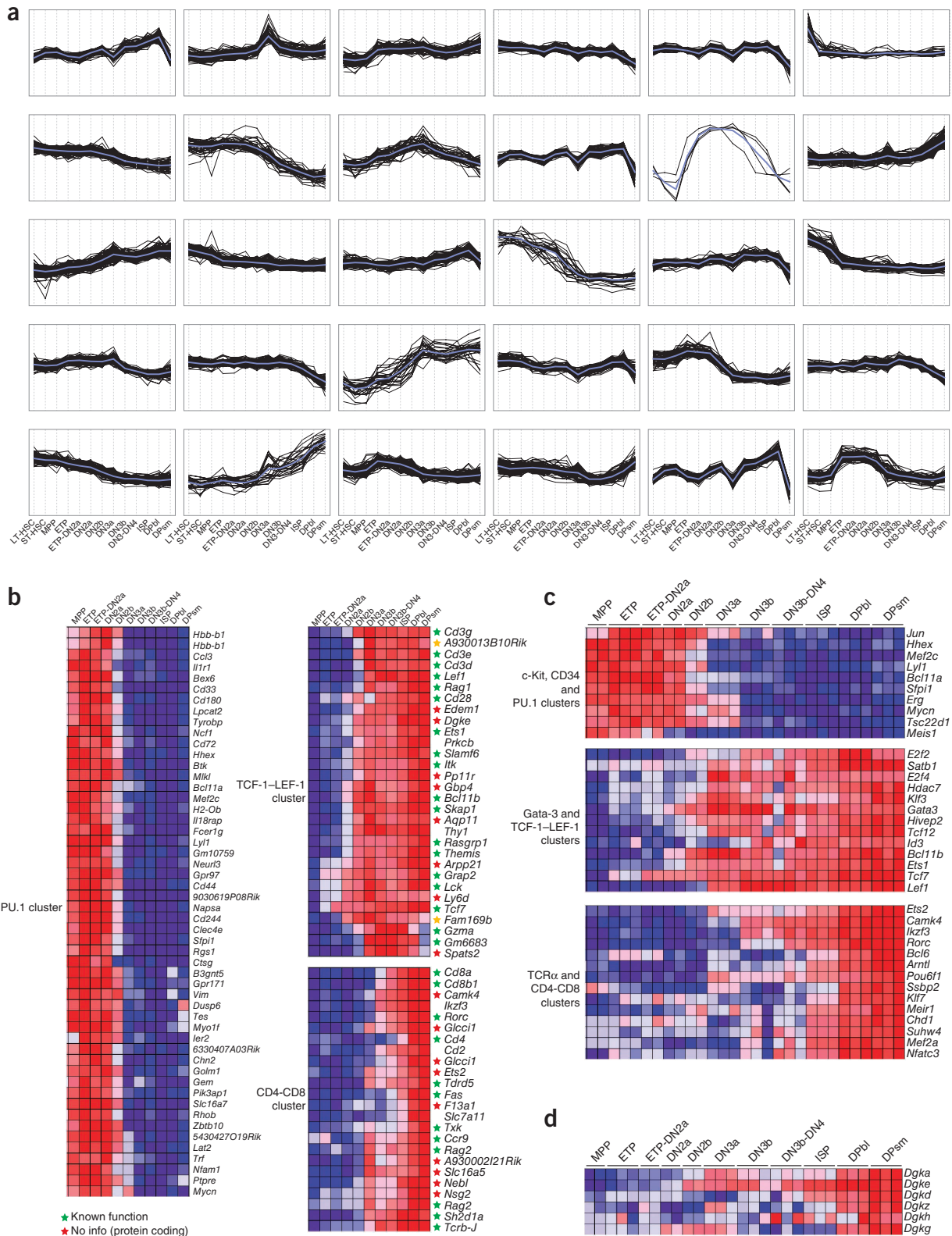


Figure 2 Dynamics of gene expression during early T cell differentiation. K-means clusters of genes with different expression profiles during early T cell differentiation. **(a)** Expression of genes (log₂-transformed mean-centered; black lines) and cluster centroids (gray line) for each cluster (named for a characteristic gene or group of genes in the cluster; complete list of genes in each, **Supplementary Table 2**). **(b)** Heat maps of the expression of genes (right margin) in the PU.1 (left), TCF-1-LEF-1 (top right) and CD4-CD8 (bottom right) clusters. **(c)** Heat maps of the expression of genes encoding transcriptional regulators (right margin) from various clusters (left margin). **(d)** Heat map of the expression of genes encoding diacylglycerol kinases (right margin) whose expression changed by threefold or more during early T cell differentiation.

© 2013 Nature America, Inc. All rights reserved. mpng

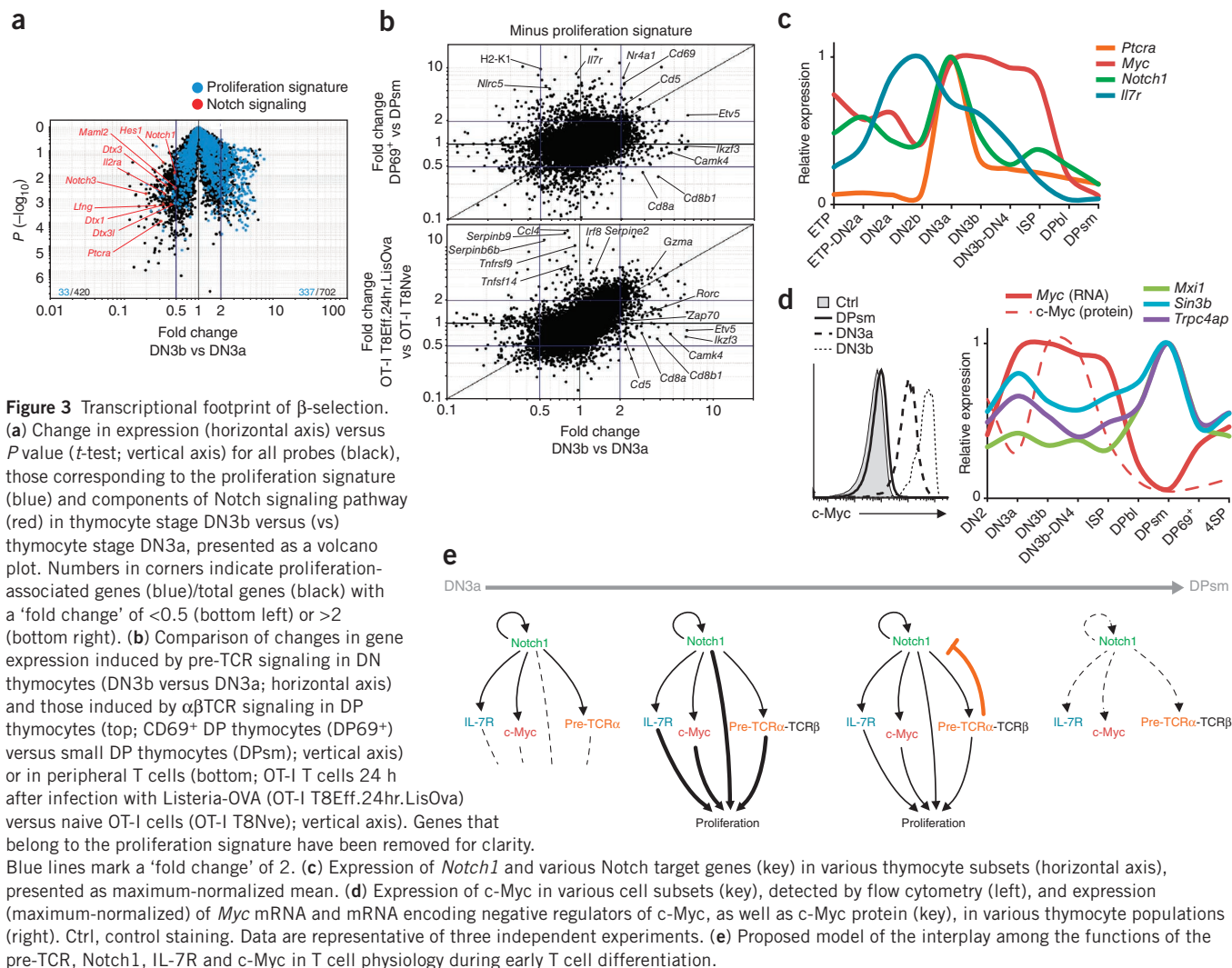


Figure 3 Transcriptional footprint of β -selection. (a) Change in expression (horizontal axis) versus P value (t -test; vertical axis) for all probes (black), those corresponding to the proliferation signature (blue) and components of Notch signaling pathway (red) in thymocyte stage DN3b versus (vs) thymocyte stage DN3a, presented as a volcano plot. Numbers in corners indicate proliferation-associated genes (blue)/total genes (black) with a 'fold change' of <0.5 (bottom left) or >2 (bottom right). (b) Comparison of changes in gene expression induced by pre-TCR signaling in DN thymocytes (DN3b versus DN3a; horizontal axis) and those induced by $\alpha\beta$ TCR signaling in DP thymocytes (top; CD69⁺ DP thymocytes (DP69⁺) versus small DP thymocytes (DPsm); vertical axis) or in peripheral T cells (bottom; OT-I T cells 24 h after infection with *Listeria*-OVA (OT-I T8Eff.24hr.LisOva) versus naive OT-I cells (OT-I T8Nve); vertical axis). Genes that belong to the proliferation signature have been removed for clarity. Blue lines mark a 'fold change' of 2. (c) Expression of *Notch1* and various Notch target genes (key) in various thymocyte subsets (horizontal axis), presented as maximum-normalized mean. (d) Expression of c-Myc in various cell subsets (key), detected by flow cytometry (left), and expression (maximum-normalized) of *Myc* mRNA and mRNA encoding negative regulators of c-Myc, as well as c-Myc protein (key), in various thymocyte populations (right). Ctrl, control staining. Data are representative of three independent experiments. (e) Proposed model of the interplay among the functions of the pre-TCR, Notch1, IL-7R and c-Myc in T cell physiology during early T cell differentiation.

in DN3 thymocytes to allow β -selection, a process that drives a burst of proliferation and phenotypic progression to the stages DN4 (with downregulation of CD25 expression), ISP (with upregulation of CD8 expression) and DP (with upregulation of the expression of both CD4 and CD8)⁵¹. Upregulation of CD28 expression is one of the earliest marks of β -selection and occurs before the complete downregulation of CD25 expression, which distinguishes post- β -selected DN3b cells from unselected DN3a cells¹². The transition from DN3a to DN3b was associated with one of the most prominent shifts in the thymocyte transcriptome (Fig. 1c–e). Much of this change was related to proliferation ($>48\%$ of upregulated genes; Fig. 3a) or metabolism (data not shown). Genes encoding known components of the β -selection program were also included in the 'TCR α ' and 'Cd4 and Cd8' clusters (for example, *Cd4*, *Cd8a*, *Cd8b1* and *Rorc*), along with genes encoding several regulators not yet recognized in the context of thymocyte differentiation (*Chd1*, *Klf7*, *Mef2a*, *Meir1*, *Pou6f1* and *Zfp280d* (which encodes Suhw4); Fig. 2b,c).

Do all TCR-mediated signals proceed similarly? We analyzed the overlap between genes induced by signaling from the pre-TCR (DN3a-to-DN3b transition) or the $\alpha\beta$ TCR in immature DP thymocytes (small DP-to-CD69⁺ DP transition) or in peripheral T cells (CD8⁺ T cells from unchallenged OT-I mice (which express an ovalbumin-specific TCR) versus those from OT-I mice challenged with ovalbumin-expressing

Listeria monocytogenes) to determine whether a common transcriptional program was engaged downstream of these receptors at various stages of T cell differentiation. Proliferation signature genes were strongly induced by both the pre-TCR at the DN3 stage and the $\alpha\beta$ TCR in peripheral T cells but not in DP thymocytes, and we therefore excluded those from this analysis (Fig. 3b). Unexpectedly, transcriptional programs induced by β -selection and peripheral T cell activation overlapped considerably, with very few genes selectively induced by the pre-TCR (those included *Rorc*, *Zap70*, *Cd8*, *Etv5* and *Ikzf3*). In contrast, TCR signaling at the DP stage seemed to be very distinct from the β -selection transcriptional program. Genes encoding several markers of TCR signal strength (*Cd69*, *Cd5* and *Nr4a1*) were induced downstream of both the pre-TCR and the $\alpha\beta$ TCR in DN and DP thymocytes, respectively, but the magnitude of their induction was lower during β -selection (Fig. 3b).

Pre-TCR signals are known to antagonize Notch signaling^{46,47}. Accordingly, genes encoding a wide array of components of the Notch pathway were downregulated after β -selection (Fig. 3a): *Notch1* and *Notch3* themselves; *Lfng*, which encodes a glycosyltransferase that enhances the sensitivity of Notch receptors to Delta-like ligands; *Maml2*, which encodes a Notch transcriptional coactivator; *Dtx1*, *Dtx3* and *Dtx3l*, which encode members of Deltex family of Notch regulators; and *Hes1*, *Il2ra*, *Ptcr* (pre-TCR α), which encode

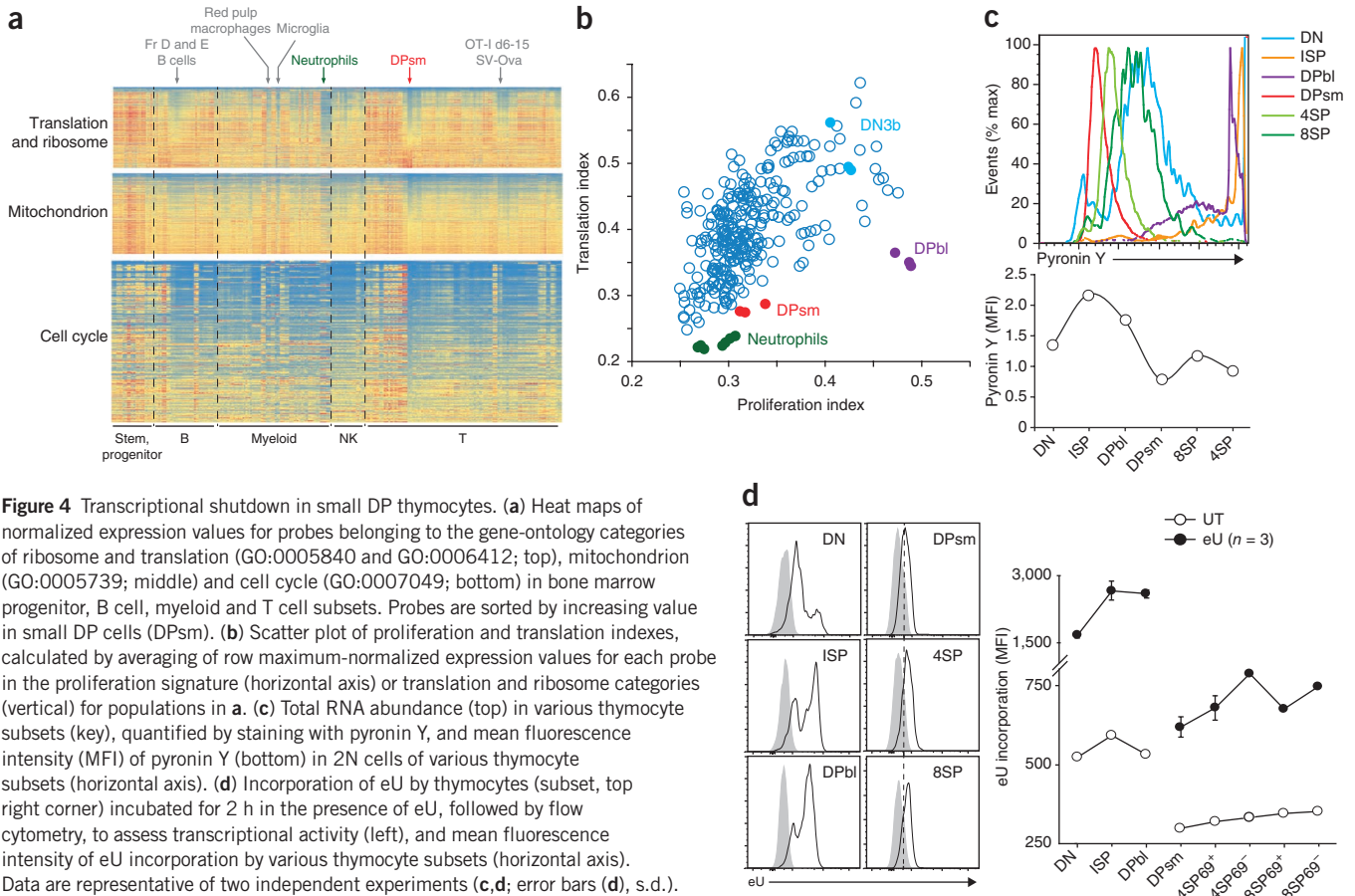


Figure 4 Transcriptional shutdown in small DP thymocytes. **(a)** Heat maps of normalized expression values for probes belonging to the gene-ontology categories of ribosome and translation (GO:0005840 and GO:0006412; top), mitochondrion (GO:0005739; middle) and cell cycle (GO:0007049; bottom) in bone marrow progenitor, B cell, myeloid and T cell subsets. Probes are sorted by increasing value in small DP cells (DPsm). **(b)** Scatter plot of proliferation and translation indexes, calculated by averaging of row maximum-normalized expression values for each probe in the proliferation signature (horizontal axis) or translation and ribosome categories (vertical) for populations in **a**. **(c)** Total RNA abundance (top) in various thymocyte subsets (key), quantified by staining with pyronin Y, and mean fluorescence intensity (MFI) of pyronin Y (bottom) in 2N cells of various thymocyte subsets (horizontal axis). **(d)** Incorporation of eU by thymocytes (subset, top right corner) incubated for 2 h in the presence of eU, followed by flow cytometry, to assess transcriptional activity (left), and mean fluorescence intensity of eU incorporation by various thymocyte subsets (horizontal axis). Data are representative of two independent experiments (c,d; error bars (d), s.d.).

Notch targets⁴⁴. Genes encoding other Notch targets, such as *Il7r*^{45,50} and *Myc*^{14,50,52}, were also downregulated at the transcriptional level, but with delayed kinetics (Fig. 3c). We also observed delayed downregulation of c-Myc protein (Fig. 3d). The abundance of c-Myc protein actually increased threefold after β -selection (Fig. 3d), in accordance with its mitogenic role at the β -selection checkpoint^{14,50,52,53}, then it was almost completely undetectable by the DP stage. We first observed this decrease in the abundance of protein at the ISP stage without a substantial decrease in mRNA (Fig. 3d), a divergence that coincided with the upregulation of the expression of genes encoding several of post-transcriptional and functional regulators of c-Myc: *Trpc4ap*, which encodes a molecule that targets c-Myc for ubiquitination⁵⁴; and *Mxi1* and *Sin3b*, which encode molecules that antagonize transactivation functions of c-Myc-MAX dimers^{55,56} (Fig. 3d). Together these observations hinted at post-transcriptional mechanisms that regulate c-Myc expression and activity.

In addition to c-Myc activity⁵³, the burst of proliferation triggered by β -selection requires signaling via both the pre-TCR and Notch^{57,58} and is augmented by signals from the receptor for interleukin 7 (IL-7R). However, pre-TCR expression shut down Notch signaling and therefore negatively regulated those mitogenic pathways. Thus, this delayed shutdown may serve as a molecular timer that sets in motion the transcriptional changes ultimately associated with transition to the quiescent small DP stage (Fig. 3e). Accordingly, when we prevented the shutdown of *Myc* expression by ectopic expression of *Myc* at the DP stage, DP thymocytes did not acquire the small cell size characteristic of the resting small DP stage (Supplementary Fig. 3a). The positive correlation between *Myc* expression and the

size of DP cells (Supplementary Fig. 3b) indicated that downregulation of *Myc* may be one of the key molecular events that drives the transition toward the quiescent small DP phenotype. Consistent with these results, both deletion of *Myc* and transgenic expression of the c-Myc inhibitor MAD1 at the DN3 stage lead to much smaller thymocytes^{53,59}.

Small DP cells

Transition from the DP blast stage to the small DP stage was associated with the greatest change to the thymocyte transcriptome. An unusual feature of this shift was that it seemed many more genes were downregulated (1,448 probes with a ‘fold change’ of <0.5) than were upregulated (225 probes with a ‘fold change’ of >2; Fig. 1e). Much of this transcriptional shutdown affected genes controlling proliferation and various ‘housekeeping’ activities such as translation, RNA processing and many metabolic processes (Supplementary Fig. 4 and data not shown). This observation was exemplified by downregulation of the ribosomal protein S6 (a part of the 40S ribosomal subunit) at the transcriptional and protein levels (Supplementary Fig. 5).

The broad shutdown of genes encoding metabolism-related molecules in small DP cells was not merely a result of exit from the cell cycle. When we simultaneously analyzed the expression of genes in the metabolism and proliferation-related gene-ontology categories across the entire ImmGen data set, many populations had the expected ‘low proliferation’ phenotype, but very few had the ‘low metabolism’ signature (Fig. 4a). Cell types that shut down their metabolism-related transcriptome to an extent similar to that of small DP cells included T cells at the contraction phase of the immune response, neutrophils,



microglia and red pulp macrophages (Fig. 4a,b). Neutrophils, like small DP thymocytes, have a lifespan of several days and have diminished transcription and translation activities and few mitochondria⁶⁰. Pre-B cells (fraction D) also underwent a similar shutdown of genes in the metabolism- and proliferation-related categories, although to a lesser extent (Fig. 4a), and like small DP cells, are on the cusp of an antigen receptor-controlled checkpoint. Given that huge numbers of cells in these subsets are destined to die because of their failure to express a 'useful' antigen receptor, acquisition of this 'low metabolism state' may be an adaptation that diminishes the energy cost of the inevitable waste in generating an adaptive immune system.

Studies have described c-Myc as a global amplifier of transcription⁶¹. Therefore, the considerable downregulation of *Myc* expression and parallel upregulation of genes encoding negative regulators of c-Myc at the small DP stage (Fig. 3d) suggested that the extent of the transcriptional shutdown may be even greater than surmised after normalization of microarray data, which assesses only relative amounts of transcripts in a cell but can miss widespread variation⁶². To test that hypothesis, we quantified total RNA by analyzing pyronin Y staining by flow cytometry (Fig. 4c). Small DP cells had less RNA than did their 'neighboring' subsets (DN, DP blast, CD4SP and CD8SP), in accord with a published report that detected 10% the amount of total RNA in small DP thymocytes relative to that in DN4 cells⁶³. We also assessed actual transcription by incorporation of the uracil analog eU (5-ethynyl uridine; Fig. 4d). An abrupt decrease in *de novo* RNA synthesis occurred at the small DP stage and was thus a major contributor to the transcriptional shutdown observed in small DP cells. Together these data indicated that RNA transcription was globally suppressed at the small DP stage and that genes encoding molecules associated with metabolic and housekeeping activities were disproportionately affected during this shutdown.

CD69⁺ DP thymocyte: crossroad of multiple fates

Small DP cells 'audition' for positive selection by scanning for self peptide-MHC interactions with their newly rearranged $\alpha\beta$ TCR⁶⁴. DP thymocytes that receive a TCR signal after engagement of peptide-MHC upregulate expression of the activation marker CD69 (ref. 65). The transition from small DP thymocyte to CD69⁺ DP thymocyte was associated with the second greatest change in the transcriptome throughout thymocyte differentiation. Accordingly, side-by-side comparison of the gene-expression profiles of CD69⁺ DP thymocytes and small DP thymocytes showed a large number of genes with different expression (Fig. 5a). As expected, a major part of the program induced in CD69⁺ DP thymocytes affected transcripts induced early in TCR activation, as shown by the distinct partitioning of the signature genes characterizing TCR-stimulated DP thymocytes (Fig. 5a). Most of those TCR-related genes (75% of the upregulated signature genes) were not DP specific, as they were shared with other examples of TCR signaling, in particular in peripheral T cells (data not shown), and thus belonged to 'generic' branches of TCR-controlled gene networks. Accordingly, a large number of immediate-early-response genes and genes encoding canonical TCR transcriptional regulators (including members of the NFAT, NF- κ B, EGR, Fos, Rel and NUR77 families) were among the upregulated signature genes (Fig. 5a).

Analysis of genes encoding transcriptional regulators that were not part of this signature (Fig. 5b) identified genes encoding molecules with possible functions in thymic positive selection. For example, the genes encoding the inhibitory molecules Id2 and Id3, proposed to relieve the differentiation blockade enforced at the DP stage by E proteins^{66–68}, were upregulated substantially in CD69⁺ DP thymocytes. Symmetrically, transcription of *Tcf12* (which encodes the transcriptional regulator HEB) was downregulated substantially (Fig. 5b and Supplementary Fig. 1).

Another hallmark of positive selection was the fourfold upregulation of *Nlrc5*, which encodes an MHC class I transactivator⁶⁹ (Fig. 5b). Although expression of MHC class I molecules was considerably impaired in *Nlrc5*-deficient mice, the increase after positive selection was largely parallel in wild-type and *Nlrc5*-deficient mice (Fig. 5c), which indicated that other factors modulate MHC class I expression at this step. Many of the other transcriptional regulators have no reported function in thymic differentiation and warrant future exploration (Fig. 5b).

Gene ontology and manual curation of the fraction of the transcriptome of CD69⁺ DP thymocytes that was not part of the 'generic' TCR-activation signature identified several other functional categories that were highly represented (Supplementary Fig. 6 and Supplementary Table 3). In particular, the 'metabolic' category represented 11% of the induced genes, with genes encoding molecules involved in several major biosynthetic and oxidative pathways. The tricarboxylic acid cycle emerged as a critical metabolic hub in the transition from small DP thymocyte to CD69⁺ DP thymocyte, with concerted transcriptional regulation of key regulators of the pyruvate dehydrogenase complex. CD69⁺ DP thymocytes downregulated genes (*Pdk1* and *Pdk2*) encoding two of the most active pyruvate dehydrogenase kinase isozymes, which catalyze the phosphorylation and inactivation of the pyruvate dehydrogenase complex, and simultaneously increased expression of genes (*Pdp1* and *Pdp2*) encoding phosphatases that catalyze the opposite reaction (Fig. 5d). In addition to that coordinated regulation of *Pdk1* and *Pdk2* with that of *Pdp1* and *Pdp2* (which is also observed in starving cells⁷⁰), CD69⁺ DP thymocytes reactivated the upstream glycolytic pathway (Fig. 5d), with upregulation of *Pgam1* (which encodes the most abundant 3-phosphoglycerate mutase in thymocytes) and downregulation of *Pgm211* (which encodes glu-1,6-biP synthase, whose reaction product negatively regulates hexokinase isozymes⁷¹).

The metabolic switch noted above was also associated with the reactivation of other cellular housekeeping activities, which together composed almost 30% of the upregulated transcriptome that was not part of the early TCR-activation signature. These included genes encoding molecules involved in the restoration of active protein synthesis (10% of upregulated genes); nucleocytoplasmic transport (2% of upregulated genes); and cytoskeleton-based motility (6% of upregulated genes; Supplementary Fig. 6 and Supplementary Table 3). One example was the upregulation of genes encoding 20 ribosome structural proteins and key regulators of translation, such as the ribosomal S6 kinase (*Rps6ka1*; Fig. 5e). Notably, for most of the genes in these categories, the upregulation was only partial at the CD69⁺ DP stage (Fig. 5e) and was completed only by the mature SP stages. Such stepwise reactivation was also reflected in cellular RNA content, as well as transcriptional rates, which increased only gradually during the differentiation of DP thymocytes into mature SP cells (Fig. 4c,d). Therefore, rather than a simple shift in the balance of pro- and antiapoptotic factors, the CD69⁺ DP stage was characterized by the reactivation of most cellular housekeeping functions downregulated at the small DP stage.

Is there evidence of negative selection in the transcriptome of CD69⁺ DP thymocytes? Although it is generally accepted that expression of CD69 identifies DP thymocytes recently engaged in positively selecting TCR-peptide-MHC interactions^{3,65}, it is not clear which (if any) fraction of CD69⁺ DP thymocytes triggered via the TCR is doomed to die after engagement of the TCR with negatively selecting peptide-MHC ligands^{72–77}. To address this question, we highlighted those genes that have been reproducibly associated with negative selection in TCR-transgenic models (*Nr4a1* (which encodes NUR77), *Bcl2l11* (which encodes Bim), *Pdcd1* (which encodes PD-1) and *Gadd45b* (which encodes GADD45B)^{29,30,78}) on a volcano plot comparing the CD69⁺ DP stage and small DP stage (Fig. 6a).

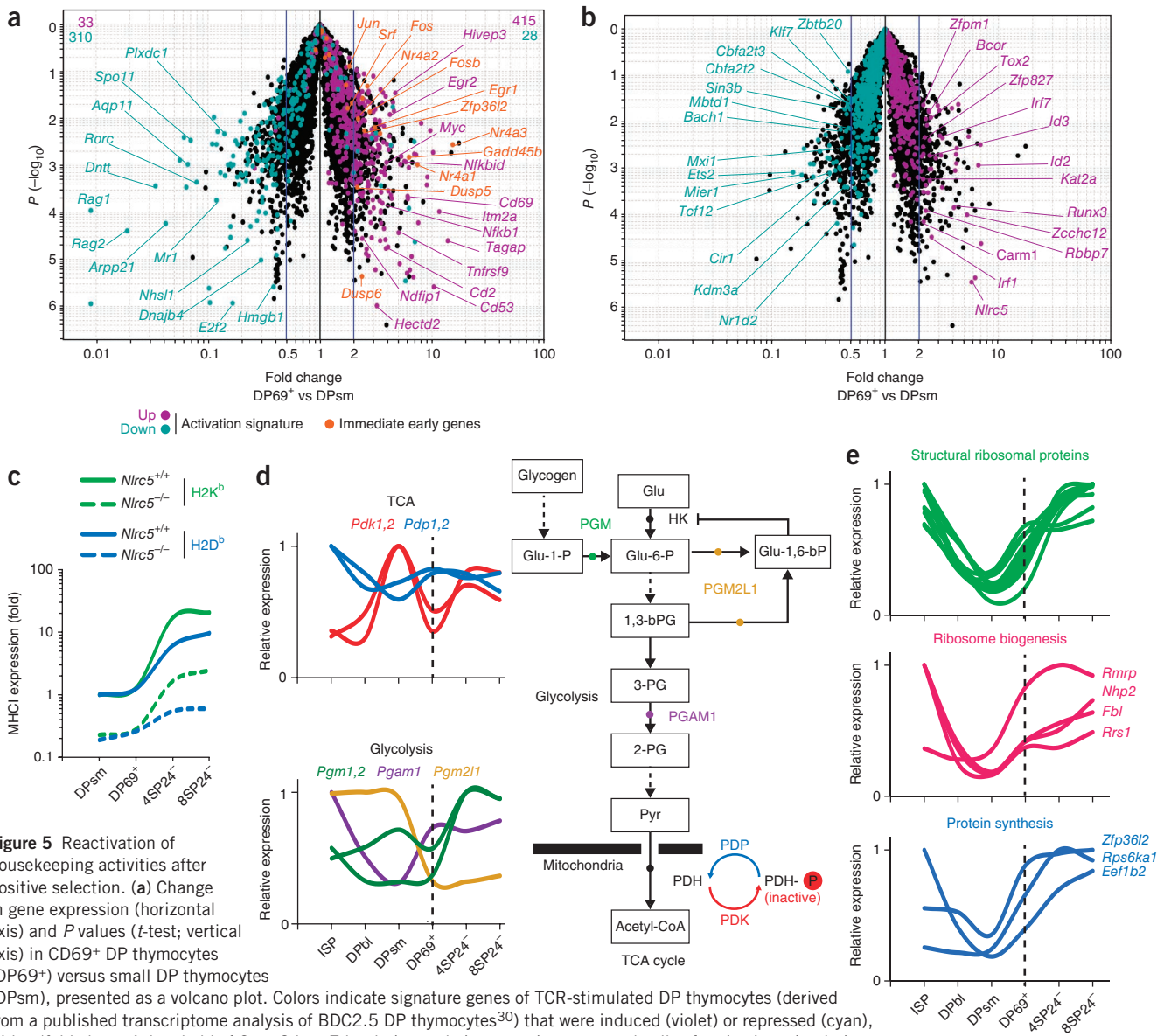


Figure 5 Reactivation of housekeeping activities after positive selection. **(a)** Change in gene expression (horizontal axis) and *P* values (*t*-test; vertical axis) in CD69⁺ DP thymocytes (DP69⁺) versus small DP thymocytes (DPsm), presented as a volcano plot. Colors indicate signature genes of TCR-stimulated DP thymocytes (derived from a published transcriptome analysis of BDC2.5 DP thymocytes³⁰) that were induced (violet) or repressed (cyan), with a 'fold change' threshold of 2, at 3 h or 7 h relative to their expression untreated cells after *in vitro* stimulation with mimotope-pulsed splenic APCs; orange indicates immediate-early-response genes (derived from transcriptome analysis of a cell line stimulated with platelet-derived growth factor⁸⁵). Numbers in top corners indicate the number of signature genes of the upregulated (violet) and downregulated (cyan) activation signatures in the induced (right) or repressed (left) quadrants. **(b)** Gene probes remaining after filtering-out of genes whose expression changed after TCR stimulation among DP signature genes (shown in **a**); colors indicate upregulated (violet) and downregulated (cyan) transcriptional regulators (among 1,680 known or putative transcriptional regulators, **Supplementary Table 4**). **(c)** Expression of MHC class I (MHCI) on various thymocyte subsets (horizontal axis) from *Nlrc5*-sufficient mice (*Nlrc5*^{+/+}) and *Nlrc5*-deficient mice (*Nlrc5*^{-/-}), detected by flow cytometry with anti-H2-K^b or anti-H2-D^b (key) and presented relative to expression in small DP thymocytes. **(d)** Expression (maximum-normalized mean) of eight metabolism-related transcripts regulated at the transition from small DP thymocyte to CD69⁺ DP thymocyte (left), whose products control key steps of the glycolytic and tricarboxylic acid (TCA) cycle pathways (right). Glu, glucose; P, phosphate; G, glycerate; Pyr, pyruvate; PDH, pyruvate dehydrogenase; HK, hexokinase. **(e)** Expression (maximum-normalized mean) of 20 genes encoding ribosomes and translation-related proteins regulated at the transition from small DP thymocyte to CD69⁺ DP thymocyte. Genes encoding structural ribosomal proteins: *Rpl3*, *Rpl37*, *Rpl38*, *Rpl39*, *Rplp1*, *Rps12*, *Rps20*, *Rps25*, *Rps28*, *Rps29*, *Rrp15* and *Rpsa*.

These genes were induced substantially in CD69⁺ DP thymocytes, which suggested that negative selection may indeed have a substantial 'footprint' on the transcriptome of CD69⁺ DP thymocytes.

To determine whether we could distinguish positive and negative selection at the transcriptional level, we next compared the transcriptomes of CD69⁺ DP thymocytes and CD4⁺CD8^{int} (intermediate CD4SP) thymocytes, which correspond to the earliest positively selected cell population that ultimately gives rise to both CD4⁺ and CD8⁺ lineages⁷ (**Fig. 6b**). As expected, most genes upregulated in

CD69⁺ DP thymocytes had similar expression in CD4⁺CD8^{int} cells (for example, *Cd53*, *Bcl2* and *H2-K1*), which confirmed that positive selection was a major contributor to the transcriptome of CD69⁺ DP thymocytes. However, a subset of the genes upregulated had higher expression in CD69⁺ DP thymocytes than in intermediate CD4SP thymocytes (for example, *Nr4a1*, *Gadd45b*, *Pdcd1* and *Bcl2l11*) or vice versa (for example, *Nlrc5*, *Il7r* and *Gimap3-Gimap4*). This divergence of the transcriptional profiles suggested putative markers associated with positive and negative selection.



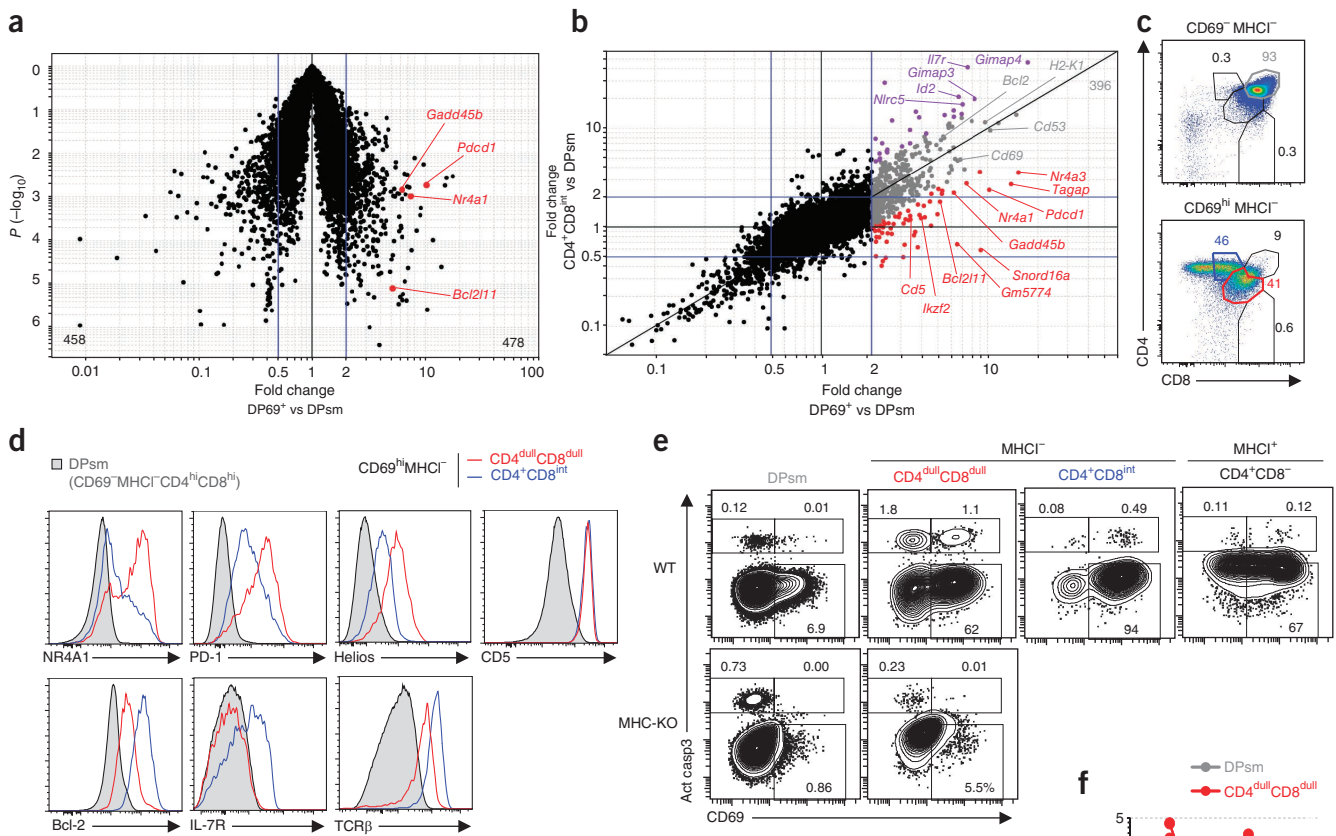


Figure 6 Transcriptional and functional ‘footprints’ of clonal deletion in CD69⁺ DP thymocytes. **(a)** Change in expression (horizontal axis) and *P* values (*t*-test; vertical axis) in CD69⁺ DP thymocytes (DP69⁺) and small DP thymocytes (DPsm), presented as a volcano plot; numbers in corners indicate total genes with a ‘fold change’ of >2 (bottom right) or <0.5 (bottom left) in CD69⁺ DP thymocytes relative to their expression in small DP; red indicates genes reproducibly associated with negative selection in TCR-transgenic models. **(b)** Comparison of gene-expression changes induced in CD69⁺ DP thymocytes (DP69⁺; horizontal axis) and intermediate thymocytes (CD4⁺CD8^{int}; vertical axis) versus small DP thymocytes (DPsm). Colors indicate genes induced over twofold in CD69⁺ DP thymocytes with greater (violet), similar (gray) or lower (red) upregulation in intermediate thymocytes (blue lines as in Fig. 3b). **(c)** Expression of CD4 and CD8 on CD69[−]MHCI[−] (top) or CD69^{hi}MHCI[−] (bottom) thymocytes (gating strategy, Supplementary Fig. 7). Numbers adjacent to outlined areas indicate percent cells in each gate. **(d)** Cell-surface expression of PD-1, IL-7R, CD5 and TCRβ and intracellular expression of Helios (IKZF2), NR4A1 and Bcl-2 by various cell subpopulations (key). **(e)** Intracellular expression of the activated, cleaved form of caspase-3 (Act casp3) and CD69 on subpopulations of cells (defined in c,d) from wild-type mice (WT) and mice doubly deficient in MHC class I and MHC class II (MHC-KO). **(f)** Proportion of cells with activated caspase-3 among various thymocyte subpopulations (key) from mice doubly deficient in MHC class I and MHC class II (MHC-KO) or Bim (Bim-KO) and their wild-type counterparts. Data are representative of three independent experiments (c,d) or one experiment (e).

We thus explored the expression of some of those markers by flow cytometry to determine whether a subset of CD69⁺ DP thymocytes was associated with apoptosis. The combined use of antibodies to MHC class I (upregulation of which was one transcriptional hallmark of positively selected cells observed in Fig. 6b; for example, *H2-K1*) and anti-CD69 subcategorized thymocytes into five distinct subpopulations (gating strategy, Supplementary Fig. 7). We were able to discern two distinct phenotypes for the CD69^{hi}MHCI[−] thymocyte fraction (Fig. 6c). The CD4^{dull}CD8^{dull} subset contained a large proportion of cells with high expression of NR4A1, PD-1 and Helios (encoded by *Ikzf2*) and little or no Bcl-2 or IL-7R (Fig. 6d). In contrast, the CD4⁺CD8^{int} subset had exactly opposite expression patterns for these markers (Fig. 6d). These results suggested that the CD4^{dull}CD8^{dull}CD69^{hi}MHCI[−] subset was enriched for cells at an early stage of deletion by apoptosis.

To test that hypothesis, we analyzed the activation of caspase-3 (Fig. 6e). Notably, the CD4^{dull}CD8^{dull} population had a singularly

high frequency of cells positive for activated caspase-3 (up to 3%), even when compared with immature SP populations, known to be sensitive to clonal deletion (Fig. 6e and Supplementary Fig. 7). Cells positive for activated caspase-3 in the CD4^{dull}CD8^{dull} population included CD69[−] cells and CD69^{hi} cells, which were much less abundant in mice doubly deficient in MHC class I and MHC class II (1–10% as many) and in Bim-deficient mice (25% as many) than in their wild-type counterparts (Fig. 6e,f). These results identified a DP thymocyte subset in unmanipulated mice that underwent cell death in an MHC- and Bim-dependent manner, which is characteristic of true clonal deletion. Small DP cell populations also contained a substantial proportion of CD69[−] cells positive for activated caspase-3 that, in contrast to the CD4^{dull}CD8^{dull} population, was larger in the absence of MHC class I and II (Fig. 6f); this probably identified cells that died by ‘neglect’. Together these observations showed an unexpectedly large deletional program in the polyclonal repertoire of DP thymocytes.



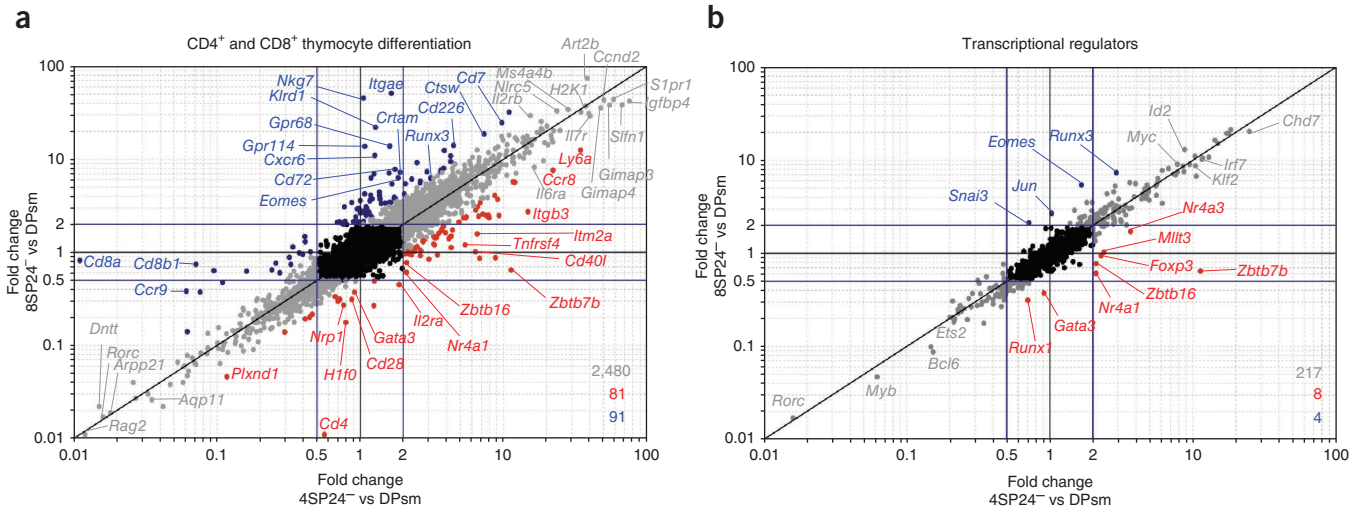


Figure 7 Acquisition of CD4⁺ and CD8⁺ transcriptional identities during thymocyte differentiation. **(a)** Comparison of gene-expression changes induced in mature CD4SP thymocytes (4SP24⁺; horizontal axis) and mature CD8SP thymocytes (8SP24⁺; vertical axis) versus small DP (DPsm). Colors indicate genes induced with similar (gray) or ‘preferential’ upregulation during CD4SP (red) or CD8SP (blue) differentiation (threshold as in **Fig. 5a**); numbers in bottom right corner indicate total genes per group (blue lines as in **Fig. 3b**). **(b)** Comparison of the gene-expression changes in **a**, filtered for a list of 1,680 known or putative transcriptional regulators (**Supplementary Table 4**).

Differentiation of CD4⁺ and CD8⁺ lineages

The results presented above indicated that the CD69⁺ DP subset was a heterogeneous population, with only a fraction of the cells differentiating from the DP stage to the SP stage. That differentiation event had one of the largest changes observed during thymocyte differentiation, with variations in the expression of more than 2,600 gene probes (**Fig. 1e** and **Fig. 7a**). Despite the scale of this transcriptome shift, most of the changes were common for both the CD4⁺ lineage and the CD8⁺ lineage (approximately 93%), with unexpectedly few genes having a difference in expression (**Fig. 7a**). Among those, *Cd40l* (which encodes the ligand for the costimulatory receptor CD40) and *Tnfrsf4* (which encodes the cell-survival factor OX40) were specifically upregulated in the CD4⁺ lineage, whereas *Crtam* and *Cd226*, which encode molecules associated with granule- and interferon- γ -mediated cytotoxic functions⁷⁹, had higher expression in the CD8⁺ lineage. Correspondingly, very few genes encoding transcriptional regulators had different expression; these were exemplified by the well-described *Zbtb7b* (which encodes Th-POK) and *Gata3* for the CD4⁺ lineage and *Runx3* and *Eomes* for the CD8⁺ lineage⁸⁰ (**Fig. 7b**). Thus, the CD4⁺ and CD8⁺ lineages were distinguished by unexpectedly few transcriptional marks during thymocyte differentiation.

Egress from the thymus is coupled with a phase of functional maturation²³. To test the hypothesis that this maturation phase could reinforce lineage identities and further demarcate their transcriptomes, we compared thymic and peripheral T cells (**Fig. 8a**). Unexpectedly, we observed little evidence of such a maturation process at the transcriptional level. Most of the downregulated genes were related to the cell cycle, which probably reflected the small fraction of proliferating mature SP thymocytes⁸¹. Only 12 genes had significant upregulation during the ‘migration’ from mature T cells to peripheral counterparts (at a ‘fold change’ threshold of 2; **Fig. 8a**). One of these genes was *Cd55*, whose product deactivates complement C3 convertases and protects cells from the lytic action of complement, whereas the function of the molecules encoded by another, *Dapl1*, is unknown in T cells. The upregulation of these genes after thymic egress was similar in the CD4⁺ and CD8⁺ lineages

(**Fig. 8a**). Finally, a small subset of genes selectively downregulated in peripheral CD4⁺ T cells reflected the inclusion of regulatory T cells in the thymic CD4⁺ subset but not the lymph node CD4⁺ subset. These observations demonstrated that egress from the thymus had limited transcriptional consequences, with no reinforcement of CD4⁺ or CD8⁺ lineage identity.

What ultimately defines lineage identity in peripheral T cells? In line with the thymocyte profiling, direct comparison of peripheral CD4⁺ or CD8⁺ T cells identified few genes with different expression (159; ‘fold change’ >2; false-discovery rate, <10⁻⁴); most of these overlapped those detected before in thymocytes (**Fig. 8b**). A few encoded molecules associated with TCR signaling functions: *Cd28*, *Trib2* (which encodes a negative regulator of mitogen-activated protein kinases) and *Mapk11* (which encodes the kinase p38 β), for CD4⁺ cells; and *Dpp4* (which encodes CD26) and *Rnf125* (a positive regulator of T cell activation), for CD8⁺ cells. Such limited divergence was unexpected, given the physiologically distinct functions of CD4⁺ T cells and CD8⁺ T cells. We reasoned that these modest differences in the baseline transcriptomes might be amplified after activation and/or reflected in post-translational cascades during activation.

Therefore, we compared TCR signaling events in CD4⁺ or CD8⁺ T cells by multidimensional mass cytometry³⁴. We stimulated suspensions of lymph node cells with antibody to CD3 (anti-CD3) and anti-CD28 and assessed the phosphorylation status of 15 intracellular signaling molecules and the expression of 7 cell surface markers at 15 time points. Despite our finding of slightly more phosphorylation in CD4⁺ T cells, most key TCR-proximal nodes (CD3 ζ , Zap70, Lat and SLP-76) and downstream nodes (Erk1/2, S6, MAPKAPKII and NF- κ B) had very similar dynamics of phosphorylation in CD4⁺ T cells and CD8⁺ T cells (**Fig. 8c**), which mirrored the transcriptional similarity. We also isolated CD4⁺ or CD8⁺ peripheral T cells and stimulated them with anti-CD3 and anti-CD28 for gene-expression profiling. Reminiscent of maturation-induced changes in thymocytes, most activation-induced changes were shared by CD4⁺ cells and CD8⁺ cells (**Fig. 8d**). Nonetheless, some divergence in the transcriptional programs of CD4⁺ cells and CD8⁺ cells was evident as early as 1 h after stimulation via the TCR and, unexpectedly, included lineage-specific

© 2013 Nature America, Inc. All rights reserved.



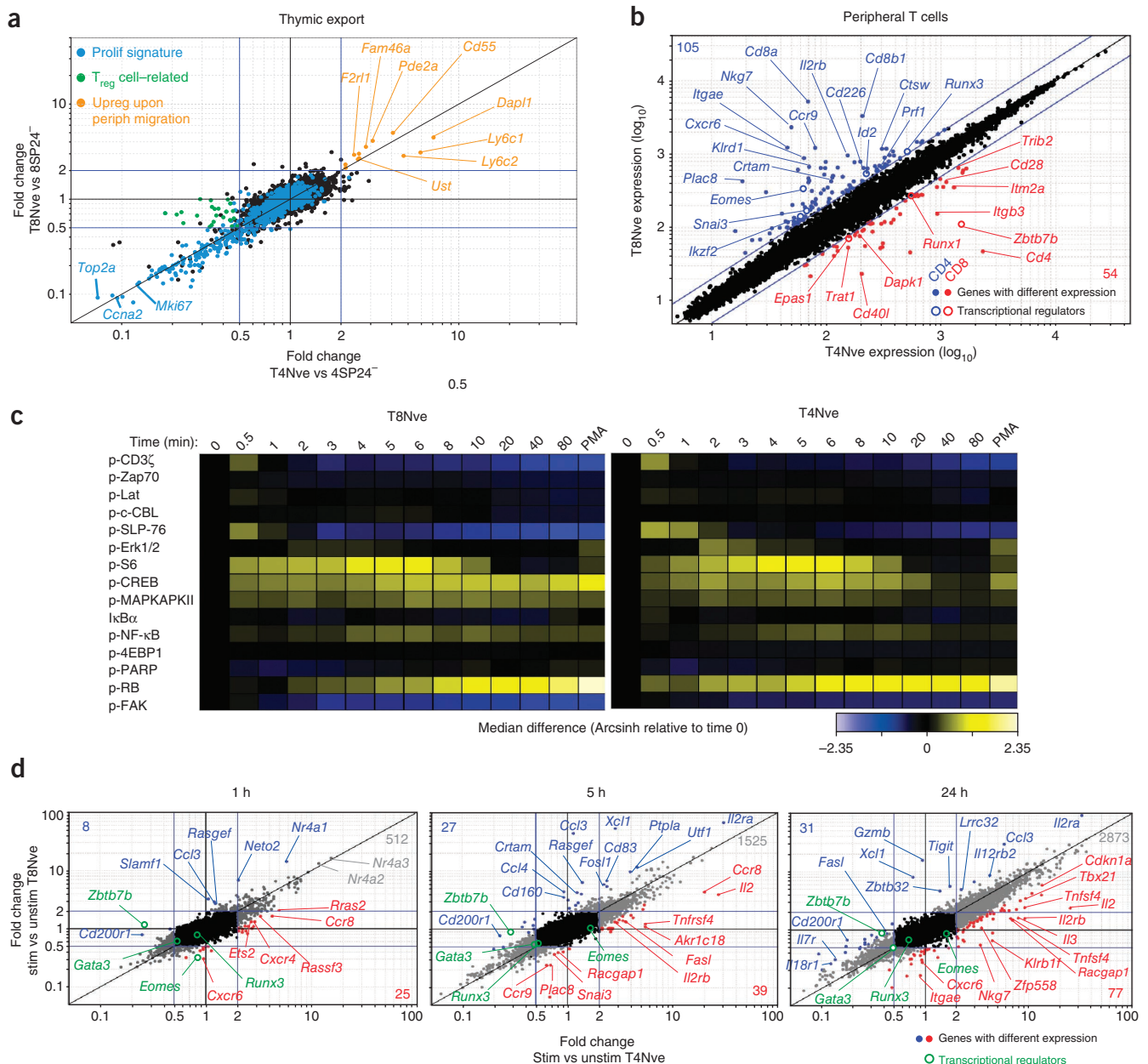


Figure 8 Definition of CD4⁺ and CD8⁺ transcriptional identities. **(a)** Comparison of gene-expression changes induced in lymph node CD4⁺ T cells (horizontal axis) and CD8⁺ T cells (vertical axis) relative to that in their thymic parental populations (mature CD4SP thymocytes (4SP24) and mature CD8SP (8SP24), respectively). Orange indicates genes upregulated by over twofold in peripheral CD4⁺ or CD8⁺ T cells relative to their thymic counterparts; green indicates regulatory T cell (T_{reg} cell)-related signature genes; blue indicates proliferation (prolif) signature (blue lines as in Fig. 3b). **(b)** Comparison of gene expression in lymph node CD4⁺ T cells (horizontal axis) and CD8⁺ T cells (vertical axis); colors indicate genes ‘preferentially’ expressed in CD4⁺ (red) or CD8⁺ (blue) T cells; numbers in top left and bottom right corners indicate total corresponding gene probes; open circles indicate genes encoding transcriptional regulators. **(c)** Heat maps of the phosphorylation (p-) of various signaling molecules (left margin) in lymph node CD8⁺ T cells (left) and CD4⁺ T cells (right), detected simultaneously by mass cytometry at multiple time points after crosslinking with anti-CD3 and anti-CD28. Far left (0), unstimulated cells; far right (PMA), cells stimulated with the phorbol ester PMA (positive control). **(d)** Comparison of gene-expression changes induced in lymph node CD4⁺ T cells (horizontal axis) and CD8⁺ T cells (vertical axis) stimulated for 1 h, 5 h or 24 h (above plots) with anti-CD3 and anti-CD28, relative to that in the corresponding unstimulated cell populations. Blue lines as in a; colors indicate genes with similar (gray) or ‘preferential’ regulation in the CD4⁺ T cell (red) or CD8⁺ T cell (blue) lineage (threshold as in Fig. 5a; numbers in corners as in b). Data are representative of four independent experiments (c).

downregulation of genes encoding the master transcriptional regulators of each lineage (*Zbtb7b*, *Gata3*, *Runx3* and *Eomes*; Fig. 8d).

The transcriptional divergence of CD4⁺ T cells and CD8⁺ T cells increased over time (Fig. 8d). One example of this was *Xcl1*, whose product attracts dendritic cells and is crucial for an efficient

cytotoxic response⁸². Other chemokine-encoding genes, such as *Ccl3* (MIP-1 α) and *Ccl4* (MIP-1 β), as well as genes encoding molecules directly involved in CD8⁺ cell functions (*Crtam* and *Gzmb*), were also selectively regulated (Fig. 8d). Genes ‘preferentially’ expressed by CD4⁺ cells included *Il2*, *Il2rb*, *Tnfrsf4* (which encodes the ligand



for OX40) and *Tnfrsf4* (which encodes OX40), among others. Therefore, the considerable similarity in the transcriptomes of the CD4⁺ and CD8⁺ lineages, acquired after positive selection, persisted through peripheral migration and was reflected in their signaling and transcriptional responses to TCR stimulation. This close transcriptional similarity is in contrast to the present perception of their very different functions.

DISCUSSION

Our analysis of the entire transcriptional spectrum of thymocyte differentiation states has provided several new insights. Dual control of *Myc* expression at the transcriptional and post-transcriptional levels (via downregulation of *Mxi1*, *Sin3b* and *Trpc4ap*) was apparent at the β -selection checkpoint and at the small DP-to-CD69⁺ DP transition, compatible with the idea that c-Myc constitutes the cellular ‘rheostat’ that enforces the programmed shutdown at the small DP stage and the reactivation of cellular functions after positive selection. Although the precise function of c-Myc at this stage remains to be investigated, several lines of evidence are in favor of this possibility. First, inhibition of c-Myc activity via overexpression of the c-Myc inhibitor MAD1 leads to smaller SP thymocytes, as well as a lower proportion of CD3^{hi} mature SP thymocytes⁵⁹. Second, although no altered phenotype has been reported in mice with overexpression or deletion of *Myc* at the DP stage in polyclonal settings^{53,83}, *Myc* overexpression in DP thymocytes from mice with transgenic expression of the MHC class I-restricted H-Y TCR leads to a greater positive selection efficiency⁸³.

The expression of a complete $\alpha\beta$ TCR renders DP thymocytes eligible for positive selection. Whether substantial negative selection also occurs at this stage in an unmanipulated, polyclonal setting has been a controversial issue. Our expression profiling has uncovered a program associated with apoptotic deletion in the early CD69⁺ DP subset, a consequence of their first TCR-peptide-MHC interactions. By tracking a variety of proteins identified through this transition, we were able to ascribe this program to a subset of CD69^{hi}MHCI⁻ DP thymocytes with activated caspase-3, which highlighted a substantial fraction of DP undergoing deletion. Further studies that take into account the dynamics of this process will be needed to more precisely quantify this early wave of cortical deletion relative to negative selection in the thymic medulla.

We have also provided here an important reference for T cell diseases such leukemia, immunodeficiency and autoimmunity. Definition of the transcriptomes of each thymocyte subset allows more precise staging of malignancies or identification of how differentiation stalls in the context of transcriptional networks. For example, T cell acute lymphoblastic leukemia induced by deficiency in the transcription factor TCF-1 is in fact driven by dysregulation of the gene encoding the transcription factor *Lef-1* (*Lef1*)⁸⁴, which emphasizes the interdependence of the transcription factors that drive early thymocyte differentiation. Furthermore, the definition of the normal dynamic of transcriptional regulation throughout thymocyte differentiation will enable the identification of the origins of network perturbations in disease-relevant models.

In conclusion, our comprehensive resolution of $\alpha\beta$ T cell transcriptomes through the entire course of their differentiation has yielded a unique perspective that colors somewhat differently the appreciation of differentiation events: the apparently gradual nature of commitment to the T cell lineage, the deep shutdown of cortical DP thymocytes followed by cellular reactivation after positive selection, and the ‘quasi-identity’ of CD4⁺ T cells and CD8⁺ T cells. We were able to take stock of the uncharted space across key transitions in thymocyte differentiation and highlight many notable candidate genes that were

as-yet-unexplored in T cells. Very few of the transcriptional regulators identified through the DP transitions have been analyzed thus far, whereas almost all of the (rare) transcription factors with different expression in CD4⁺ T cells versus CD8⁺ T cells have already been characterized. Thus, our analysis has defined the ‘known unknowns’ in $\alpha\beta$ T cell differentiation, and the challenge now is to integrate those with the known facts for a more complete view of T cell biology.

METHODS

Methods and any associated references are available in the [online version of the paper](#).

Accession codes. GEO: microarray data, [GSE15907](#).

Note: Supplementary information is available in the online version of the paper.

ACKNOWLEDGMENTS

We thank K. Hattori, A. Ortiz-Lopez and N. Asinovski for technical assistance with mice and antibodies; J. Moore and A. Kressler for flow cytometry; and C. Laplace for assistance with figure preparation. Supported by the US National Institutes of Health (AI072073), the Human Frontier Science Program (HFSP-LT000096 to M.M.), the National Health and Medical Research Council (637353 to D.G.) and the Australian Research Council (LP110201169 to, T.H.).

AUTHOR CONTRIBUTIONS

M.M., T.K., D.G. and T.H. designed, did and analyzed some of the experiments and wrote the manuscript; R.C. and J.E. helped with microarray data analysis; S.B. and M.H.S. designed, did and analyzed some of the experiments; G.P.N. and K.K. and H.v.B. contributed resources and assisted with data analysis; and D.M. and C.B. directed the study, analyzed and interpreted results and wrote the manuscript.

COMPETING FINANCIAL INTERESTS

The authors declare no competing financial interests.

Reprints and permissions information is available online at <http://www.nature.com/reprints/index.html>.

1. Miller, J.F. The golden anniversary of the thymus. *Nat. Rev. Immunol.* **11**, 489–495 (2011).
2. von Boehmer, H., Teh, H.S. & Kisielow, P. The thymus selects the useful, neglects the useless and destroys the harmful. *Immunol. Today* **10**, 57–61 (1989).
3. Jameson, S.C., Hogquist, K.A. & Bevan, M.J. Positive selection of thymocytes. *Annu. Rev. Immunol.* **13**, 93–126 (1995).
4. Robey, E. Regulation of T cell fate by Notch. *Annu. Rev. Immunol.* **17**, 283–295 (1999).
5. Hogquist, K.A., Baldwin, T.A. & Jameson, S.C. Central tolerance: learning self-control in the thymus. *Nat. Rev. Immunol.* **5**, 772–782 (2005).
6. Strylesky, G.L., Jameson, S.C. & Hogquist, K.A. Selection of self-reactive T cells in the thymus. *Annu. Rev. Immunol.* **30**, 95–114 (2012).
7. Singer, A., Adoro, S. & Park, J.H. Lineage fate and intense debate: myths, models and mechanisms of CD4- versus CD8-lineage choice. *Nat. Rev. Immunol.* **8**, 788–801 (2008).
8. Thompson, P.K. & Zuniga-Pflucker, J.C. On becoming a T cell, a convergence of factors kick it up a notch along the way. *Semin. Immunol.* **23**, 350–359 (2011).
9. Rothenberg, E.V. T cell lineage commitment: identity and renunciation. *J. Immunol.* **186**, 6649–6655 (2011).
10. Godfrey, D.I., Kennedy, J., Suda, T. & Zlotnik, A. A developmental pathway involving four phenotypically and functionally distinct subsets of CD3-CD4-CD8- triple-negative adult mouse thymocytes defined by CD44 and CD25 expression. *J. Immunol.* **150**, 4244–4252 (1993).
11. Bhandoola, A., von, B.H., Petrie, H.T. & Zuniga-Pflucker, J.C. Commitment and developmental potential of extrathymic and intrathymic T cell precursors: plenty to choose from. *Immunity* **26**, 678–689 (2007).
12. Williams, J.A. *et al.* Regulated costimulation in the thymus is critical for T cell development: dysregulated CD28 costimulation can bypass the pre-TCR checkpoint. *J. Immunol.* **175**, 4199–4207 (2005).
13. Prinz, I. *et al.* Visualization of the earliest steps of $\gamma\delta$ T cell development in the adult thymus. *Nat. Immunol.* **7**, 995–1003 (2006).
14. Kreslavsky, T. *et al.* β -Selection-induced proliferation is required for $\alpha\beta$ T cell differentiation. *Immunity* **37**, 840–853 (2012).
15. Zinkernagel, R.M., Callahan, G.N., Klein, J. & Dennert, G. Cytotoxic T cells learn specificity for self H-2 during differentiation in the thymus. *Nature* **271**, 251–253 (1978).
16. MacDonald, H.R. *et al.* Positive selection of CD4⁺ thymocytes controlled by MHC class II gene products. *Nature* **336**, 471–473 (1988).
17. Kisielow, P., Teh, H.S., Bluthmann, H. & von Boehmer, H. Positive selection of antigen-specific T cells in thymus by restricting MHC molecules. *Nature* **335**, 730–733 (1988).

18. Bousoo, P., Bhakta, N.R., Lewis, R.S. & Robey, E. Dynamics of thymocyte-stromal cell interactions visualized by two-photon microscopy. *Science* **296**, 1876–1880 (2002).
19. Egerton, M., Scollay, R. & Shortman, K. Kinetics of mature T-cell development in the thymus. *Proc. Natl. Acad. Sci. USA* **87**, 2579–2582 (1990).
20. Teh, H.S. *et al.* Thymic major histocompatibility complex antigens and the $\alpha\beta$ T-cell receptor determine the CD4/CD8 phenotype of T cells. *Nature* **335**, 229–233 (1988).
21. Jordan, M.S. *et al.* Thymic selection of CD4⁺CD25⁺ regulatory T cells induced by an agonist self-peptide. *Nat. Immunol.* **2**, 301–306 (2001).
22. Leishman, A.J. *et al.* Precursors of functional MHC class I- or class II-restricted CD8 $\alpha\alpha$ ⁺ T cells are positively selected in the thymus by agonist self-peptides. *Immunity* **16**, 355–364 (2002).
23. Fink, P.J. & Hendricks, D.W. Post-thymic maturation: young T cells assert their individuality. *Nat. Rev. Immunol.* **11**, 544–549 (2011).
24. DeRyckere, D., Mann, D.L. & DeGregori, J. Characterization of transcriptional regulation during negative selection *in vivo*. *J. Immunol.* **171**, 802–811 (2003).
25. Schmitz, I., Clayton, L.K. & Reinherz, E.L. Gene expression analysis of thymocyte selection *in vivo*. *Int. Immunol.* **15**, 1237–1248 (2003).
26. Liston, A. *et al.* Generalized resistance to thymic deletion in the NOD mouse; a polygenic trait characterized by defective induction of Bim. *Immunity* **21**, 817–830 (2004).
27. Mick, V.E. *et al.* The regulated expression of a diverse set of genes during thymocyte positive selection *in vivo*. *J. Immunol.* **173**, 5434–5444 (2004).
28. Zucchelli, S. *et al.* Defective central tolerance induction in NOD mice: genomics and genetics. *Immunity* **22**, 385–396 (2005).
29. Baldwin, T.A. & Hogquist, K.A. Transcriptional analysis of clonal deletion *in vivo*. *J. Immunol.* **179**, 837–844 (2007).
30. Mingueneau, M. *et al.* Thymic negative selection is functional in NOD mice. *J. Exp. Med.* **209**, 623–637 (2012).
31. Zhang, J.A. *et al.* Dynamic transformations of genome-wide epigenetic marking and transcriptional control establish T cell identity. *Cell* **149**, 467–482 (2012).
32. Li, L., Leid, M. & Rothenberg, E.V. An early T cell lineage commitment checkpoint dependent on the transcription factor Bcl11b. *Science* **329**, 89–93 (2010).
33. Luc, S. *et al.* The earliest thymic T cell progenitors sustain B cell and myeloid lineage potential. *Nat. Immunol.* **13**, 412–419 (2012).
34. Bendall, S.C. *et al.* Single-cell mass cytometry of differential immune and drug responses across a human hematopoietic continuum. *Science* **332**, 687–696 (2011).
35. Narayan, K. *et al.* Intrathymic programming of effector fates in three molecularly distinct $\gamma\delta$ T cell subtypes. *Nat. Immunol.* **13**, 511–518 (2012).
36. Ikawa, T. *et al.* An essential developmental checkpoint for production of the T cell lineage. *Science* **329**, 93–96 (2010).
37. Li, P. *et al.* Reprogramming of T cells to natural killer-like cells upon Bcl11b deletion. *Science* **329**, 85–89 (2010).
38. Rothenberg, E.V., Zhang, J. & Li, L. Multilayered specification of the T-cell lineage fate. *Immunol. Rev.* **238**, 150–168 (2010).
39. Rakhilin, S.V. *et al.* A network of control mediated by regulator of calcium/calmodulin-dependent signaling. *Science* **306**, 698–701 (2004).
40. Kisielow, J., Nairn, A.C. & Karjalainen, K. TARPP, a novel protein that accompanies TCR gene rearrangement and thymocyte education. *Eur. J. Immunol.* **31**, 1141–1149 (2001).
41. Olenchok, B.A. *et al.* Disruption of diacylglycerol metabolism impairs the induction of T cell energy. *Nat. Immunol.* **7**, 1174–1181 (2006).
42. Guo, R. *et al.* Synergistic control of T cell development and tumor suppression by diacylglycerol kinase α and ζ . *Proc. Natl. Acad. Sci. USA* **105**, 11909–11914 (2008).
43. Deftos, M.L. *et al.* Notch1 signaling promotes the maturation of CD4 and CD8 SP thymocytes. *Immunity* **13**, 73–84 (2000).
44. Reizis, B. & Leder, P. Direct induction of T lymphocyte-specific gene expression by the mammalian Notch signaling pathway. *Genes Dev.* **16**, 295–300 (2002).
45. González-García, S. *et al.* CSL-MAML-dependent Notch1 signaling controls T lineage-specific IL-7R α gene expression in early human thymopoiesis and leukemia. *J. Exp. Med.* **206**, 779–791 (2009).
46. Yashiro-Ohtani, Y. *et al.* Pre-TCR signaling inactivates Notch1 transcription by antagonizing E2A. *Genes Dev.* **23**, 1665–1676 (2009).
47. Taghon, T. *et al.* Developmental and molecular characterization of emerging β - and $\gamma\delta$ -selected pre-T cells in the adult mouse thymus. *Immunity* **24**, 53–64 (2006).
48. Gernar, K. *et al.* T-cell factor 1 is a gatekeeper for T-cell specification in response to Notch signaling. *Proc. Natl. Acad. Sci. USA* **108**, 20060–20065 (2011).
49. Weber, B.N. *et al.* A critical role for TCF-1 in T-lineage specification and differentiation. *Nature* **476**, 63–68 (2011).
50. Weng, A.P. *et al.* c-Myc is an important direct target of Notch1 in T-cell acute lymphoblastic leukemia/lymphoma. *Genes Dev.* **20**, 2096–2109 (2006).
51. von Boehmer, H. Selection of the T-cell repertoire: receptor-controlled checkpoints in T-cell development. *Adv. Immunol.* **84**, 201–238 (2004).
52. Wong, G.W. *et al.* HES1 opposes a PTEN-dependent check on survival, differentiation, and proliferation of TCR β -selected mouse thymocytes. *Blood* **120**, 1439–1448 (2012).
53. Dose, M. *et al.* c-Myc mediates pre-TCR-induced proliferation but not developmental progression. *Blood* **108**, 2669–2677 (2006).
54. Choi, S.H., Wright, J.B., Gerber, S.A. & Cole, M.D. Myc protein is stabilized by suppression of a novel E3 ligase complex in cancer cells. *Genes Dev.* **24**, 1236–1241 (2010).
55. Adhikary, S. & Eilers, M. Transcriptional regulation and transformation by Myc proteins. *Nat. Rev. Mol. Cell Biol.* **6**, 635–645 (2005).
56. Schreiber-Agus, N. & DePinho, R.A. Repression by the Mad(Mxi1)-Sin3 complex. *Bioessays* **20**, 808–818 (1998).
57. Ciofani, M. *et al.* Obligatory role for cooperative signaling by pre-TCR and Notch during thymocyte differentiation. *J. Immunol.* **172**, 5230–5239 (2004).
58. Maillard, I. *et al.* The requirement for Notch signaling at the β -selection checkpoint *in vivo* is absolute and independent of the pre-T cell receptor. *J. Exp. Med.* **203**, 2239–2245 (2006).
59. Iritani, B.M. *et al.* Modulation of T-lymphocyte development, growth and cell size by the Myc antagonist and transcriptional repressor Mad1. *EMBO J.* **21**, 4820–4830 (2002).
60. Geering, B. & Simon, H.U. Peculiarities of cell death mechanisms in neutrophils. *Cell Death Differ.* **18**, 1457–1469 (2011).
61. Nie, Z. *et al.* c-Myc is a universal amplifier of expressed genes in lymphocytes and embryonic stem cells. *Cell* **151**, 68–79 (2012).
62. Lovén, J. *et al.* Revisiting global gene expression analysis. *Cell* **151**, 476–482 (2012).
63. Neilson, J.R., Zheng, G.X., Burge, C.B. & Sharp, P.A. Dynamic regulation of miRNA expression in ordered stages of cellular development. *Genes Dev.* **21**, 578–589 (2007).
64. Starr, T.K., Jameson, S.C. & Hogquist, K.A. Positive and negative selection of T cells. *Annu. Rev. Immunol.* **21**, 139–176 (2003).
65. Swat, W., Dessing, M., von, B.H. & Kisielow, P. CD69 expression during selection and maturation of CD4⁺8⁺ thymocytes. *Eur. J. Immunol.* **23**, 739–746 (1993).
66. Jones, M.E. & Zhuang, Y. Acquisition of a functional T cell receptor during T lymphocyte development is enforced by HEB and E2A transcription factors. *Immunity* **27**, 860–870 (2007).
67. Rivera, R.R. *et al.* Thymocyte selection is regulated by the helix-loop-helix inhibitor protein, Id3. *Immunity* **12**, 17–26 (2000).
68. Bain, G. *et al.* Regulation of the helix-loop-helix proteins, E2A and Id3, by the Ras-ERK MAPK cascade. *Nat. Immunol.* **2**, 165–171 (2001).
69. Meissner, T.B. *et al.* NLR family member NLRC5 is a transcriptional regulator of MHC class I genes. *Proc. Natl. Acad. Sci. USA* **107**, 13794–13799 (2010).
70. Huang, B., Wu, P., Popov, K.M. & Harris, R.A. Starvation and diabetes reduce the amount of pyruvate dehydrogenase phosphatase in rat heart and kidney. *Diabetes* **52**, 1371–1376 (2003).
71. Maliekal, P. *et al.* Molecular identification of mammalian phosphopentomutase and glucose-1,6-bisphosphate synthase, two members of the α -D-phosphohexomutase family. *J. Biol. Chem.* **282**, 31844–31851 (2007).
72. van Meerwijk, J.P. *et al.* Quantitative impact of thymic clonal deletion on the T cell repertoire. *J. Exp. Med.* **185**, 377–383 (1997).
73. Surh, C.D. & Sprent, J. T-cell apoptosis detected *in situ* during positive and negative selection in the thymus. *Nature* **372**, 100–103 (1994).
74. Viret, C. *et al.* A role for accessibility to self-peptide-self-MHC complexes in intrathymic negative selection. *J. Immunol.* **166**, 4429–4437 (2001).
75. McCaughy, T.M., Baldwin, T.A., Wilken, M.S. & Hogquist, K.A. Clonal deletion of thymocytes can occur in the cortex with no involvement of the medulla. *J. Exp. Med.* **205**, 2575–2584 (2008).
76. Baldwin, K.K., Trenchak, B.P., Altman, J.D. & Davis, M.M. Negative selection of T cells occurs throughout thymic development. *J. Immunol.* **163**, 689–698 (1999).
77. Krueger, A. & von Boehmer, H. Identification of a T lineage-committed progenitor in adult blood. *Immunity* **26**, 105–116 (2007).
78. Liston, A. *et al.* Impairment of organ-specific T cell negative selection by diabetes susceptibility genes: genomic analysis by mRNA profiling. *Genome Biol.* **8**, R12 (2007).
79. Chan, C.J., Andrews, D.M. & Smyth, M.J. Receptors that interact with nectin and nectin-like proteins in the immunosurveillance and immunotherapy of cancer. *Curr. Opin. Immunol.* **24**, 246–251 (2012).
80. Wang, L. & Bosselut, R. CD4–CD8 lineage differentiation: Thpok-ing into the nucleus. *J. Immunol.* **183**, 2903–2910 (2009).
81. Pénit, C. & Vasseur, F. Expansion of mature thymocyte subsets before emigration to the periphery. *J. Immunol.* **159**, 4848–4856 (1997).
82. Lei, Y. & Takahama, Y. XCL1 and XCR1 in the immune system. *Microbes Infect.* **14**, 262–267 (2012).
83. Rudolph, B., Hueber, A.O. & Evan, G.I. Reversible activation of c-Myc in thymocytes enhances positive selection and induces proliferation and apoptosis *in vitro*. *Oncogene* **19**, 1891–1900 (2000).
84. Yu, S. *et al.* The TCF-1 and LEF-1 transcription factors have cooperative and opposing roles in T cell development and malignancy. *Immunity* **37**, 813–826 (2012).
85. Tullai, J.W. *et al.* Immediate-early and delayed primary response genes are distinct in function and genomic architecture. *J. Biol. Chem.* **282**, 23981–23995 (2007).

The complete list of authors is as follows: Adam J Best¹⁰, Jamie Knell¹⁰, Ananda Goldrath¹⁰, Vladimir Jojic¹¹, Daphne Koller¹¹, Tal Shay¹², Aviv Regev¹², Nadia Cohen¹³, Patrick Brennan¹³, Michael Brenner¹³, Francis Kim¹⁴, Tata Nageswara Rao¹⁴, Amy Wagers¹⁴, Tracy Heng¹, Jeffrey Ericson¹, Katherine Rothamel¹, Adriana Ortiz-Lopez¹, Diane Mathis¹, Christophe Benoist¹, Natalie A Bezman¹⁵, Joseph C Sun¹⁵, Gundula Min-Oo¹⁵, Charlie C Kim¹⁵, Lewis L Lanier¹⁵, Jennifer Miller¹⁶, Brian Brown¹⁶, Miriam Merad¹⁶, Emmanuel L Gautier^{16,17}, Claudia Jakubzick¹⁶, Gwendalyn J Randolph^{16,17}, Paul Monach¹⁸, David A Blair¹⁹, Michael L Dustin¹⁹, Susan A Shinton²⁰, Richard R Hardy²⁰, David Laidlaw²¹, Jim Collins²², Roi Gazit²³, Derrick J Rossi²³, Nidhi Malhotra²⁴, Katelyn Sylvia²⁴, Joonsoo Kang²⁴, Taras Kreslavsky²⁵, Anne Fletcher²⁵, Kutlu Elpek²⁵, Angeliq ue Bellemare-Pelletier²⁵, Deepali Malhotra²⁵ & Shannon Turley²⁵

¹⁰Division of Biological Sciences, University of California San Diego, La Jolla, California, USA. ¹¹Computer Science Department, Stanford University, Stanford, California, USA. ¹²Broad Institute and Department of Biology, MIT, Cambridge, Massachusetts, USA. ¹³Division of Rheumatology, Immunology and Allergy, Brigham and Women's Hospital, Boston, Massachusetts, USA. ¹⁴Joslin Diabetes Center, Boston, Massachusetts, USA. ¹⁵Department of Microbiology & Immunology, University of California San Francisco, San Francisco, California, USA. ¹⁶Icahn Medical Institute, Mount Sinai Hospital, New York, New York, USA. ¹⁷Department of Pathology & Immunology, Washington University, St. Louis, Missouri, USA. ¹⁸Department of Medicine, Boston University, Boston, Massachusetts, USA. ¹⁹Skirball Institute of Biomolecular Medicine, New York University School of Medicine, New York, New York, USA. ²⁰Fox Chase Cancer Center, Philadelphia, Pennsylvania, USA. ²¹Computer Science Department, Brown University, Providence, Rhode Island, USA. ²²Department of Biomedical Engineering, Howard Hughes Medical Institute, Boston University, Boston, Massachusetts, USA. ²³Program in Molecular Medicine, Children's Hospital, Boston, Massachusetts, USA. ²⁴Department of Pathology, University of Massachusetts Medical School, Worcester, Massachusetts, USA. ²⁵Dana-Farber Cancer Institute and Harvard Medical School, Boston, Massachusetts, USA.

ONLINE METHODS

Mice. Male C57BL/6J mice 6 weeks of age (The Jackson Laboratory) were maintained in specific pathogen-free conditions (protocol 02954 of the Harvard Medical School Institutional Animal Care and Use Committee). Cells were obtained from mice within 1 week of arrival according to ImmGen standard operating protocol. Mice deficient in MHC or Bim have been described⁸⁶.

Antibodies. The following monoclonal antibodies were used for flow cytometry: monoclonal antibody (mAb) to CD19 (1D3), mAb to c-Kit (2B8), mAb to CD44 (IM7), mAb to CD25 (PC61), mAb to CD4 (RM4-5), mAb to TCR β (H57-597), mAb to TCR $\gamma\delta$ (GL3), mAb to CD11b (M1/70), mAb to CD11c (N418), mAb to -NK1.1 (PK136), mAb to Gr-1 (RB6-8C5), mAb to Ter-119 (Ter-119), mAb to H-2K^b (AF6-88.5), mAb to H-2D^b (KH95), mAb to CD69 (H1.2F3), mAb to CD5 (53-7.3), mAb to CD279 (anti-PD-1; 29F.1A12; all from Biolegend); mAb to CD8 α (53-6.7) and mAb to CD127 (A7R34; all from eBioscience); and mAb to Bcl-2 (BCL10C4), mAb to IKZF2 (22.F6), mAb to NR4A1 (12.14), mAb to cleaved caspase-3 (5A1E), mAb to c-Myc (D84C12) and mAb to RPS6 (54D2; all from Cell Signaling). Primary conjugates of the following antibodies for mass cytometry were prepared and titrated as described⁸⁷: mAb to CD4 (RMA4-5), mAb to CD8 (53-6.7) and mAb to CD5 (53-7.3; all from Biolegend); mAb to Erk1/2 phosphorylated at Thr202 and Tyr204 (197G2), mAb to MAPKAPKII phosphorylated at Thr334 (27B7), rabbit polyclonal antibody to FAK phosphorylated at Tyr397 (3283), mAb to I κ B α (L35A5), mAb to CREB phosphorylated at Ser133 (87G3) and mAb to 4EBP1 phosphorylated at Thr37 and Thr46 (236B4; all from Cell Signaling); and mAb to CD19 (1D3), mAb to TCR β (H57-597), mAb to CD25 (3C7), mAb to CD44 (IM7), mAb to CD3 ζ phosphorylated at Tyr142 (K25-407.69), mAb to Zap70 phosphorylated at Tyr319 and Tyr352 (17a), mAb to Lat phosphorylated at Tyr226 (J96-1238.58.93), mAb to SLP-76 phosphorylated at Tyr128 (J141-668.36.58), mAb to c-Cbl phosphorylated at Tyr700 (47), mAb to S6 phosphorylated at Ser 235 and Ser236 (N7-548), mAb to NF- κ B phosphorylated at Ser529 (K10-895.12-50) and mAb to Rb phosphorylated at Ser807 and Ser811 (J112-906; all from BD Biosciences).

Flow cytometry and cell isolation. For surface staining, cells were incubated for 20 min at 4 °C with antibodies (identified above). For intracellular staining, cells were labeled with antibodies to surface markers (identified above), then were fixed and made permeable with Cytotfix/Cytoperm and Perm/Wash buffers (BD Pharmingen). Cells were then stained for 30 min at 4 °C with antibodies diluted in Perm/Wash buffer. For intracellular detection of c-Myc, IKZF2, NR4A1 and Bcl-2, Foxp3 fixation and permeabilization solutions from eBioscience were used. An LSR II and FACSAria (BD) were used for multiparameter analysis of stained cell suspensions, followed by analysis with FlowJo software (Tree Star). For cell sorting, cells were prepared according to the standardized ImmGen sorting protocol (http://www.immgen.org/Protocols/ImmGen_Cell_prep_and_sorting_SOP.pdf) with the appropriate antibodies (identified above). Cells were sorted on a FACSAria and FACSAria II (BD). The marker combinations used for the sorting of specific populations are available on the ImmGen website. For the isolation of DN thymocyte subpopulations, total thymocytes were enriched for lineage-negative cells by staining of cell suspensions with biotinylated anti-CD4 (RM4-5), anti-CD8a (53-6.7), anti-TCR β (H57-597), anti-TCR $\gamma\delta$ (GL3), anti-CD11b (M1/70), anti-CD11c (N418), anti-NK1.1 (PK136), anti-Gr-1 (RB6-8C5) and anti-Ter-119 (TER-119; all from Biolegend), followed by incubation with streptavidin-conjugated M-280 magnetic beads (Dyna/Invitrogen) and magnetic bead depletion of lineage-positive cells. Fluorochrome-conjugated streptavidin was added to the staining 'cocktail' and the remaining lineage-positive cells were gated out electronically.

RNA measurement. For pyronin Y staining, freshly isolated thymocytes were labeled with antibody conjugate to cell surface proteins (antibodies identified above), then were washed and fixed in fixation/permeabilization reagent according to manufacturer's instructions (BD Biosciences). Cells were washed in permeabilization/wash solution, then were stained for 10 min with 2.5 μ g/ml DAPI (4,6-diamidino-2-phenylindole; Molecular Probes). Cells were washed and resuspended in 1 μ g/ml pyronin Y (Sigma Aldrich) and incubated for 10 min, then were acquired on an LSRII (BD) with linear scales for pyronin Y

and DAPI channels. Transcriptional activity was measured in freshly isolated thymocytes during 2 h of incubation at 37 °C in presence of 5 mM eU. Cells were collected, stained for extracellular antigens (antibodies identified above) and then processed for eU detection by click chemistry according to manufacturer's instructions (Invitrogen).

Cell stimulation. For gene-expression profiling of activated CD4⁺ T cells and CD8⁺ T cells, sorted naive CD4⁺ T cells and CD8⁺ T cells were cultured together with beads coated with anti-CD3 and anti-28 (cells/beads, 1:0.4; Dynabeads mouse T-activator; Dynal) and were collected at various time points after stimulation by cell sorting. For analysis of phosphorylation events by mass cytometry, total lymph node cells were stimulated in medium containing 6 μ g/ml of biotinylated anti-CD3 ϵ (145-2C11; Biolegend) and anti-CD28 (37.51; Biolegend) and were incubated for 2 min at 37 °C before the addition of 24 μ g/ml streptavidin. At various times after crosslinking, cells were fixed by the addition of paraformaldehyde (final concentration 2%). PMA controls were fixed 3 min after the addition of 10 ng/ml PMA (phorbol 12-myristate 13-acetate).

OP9-DL1 cultures and retroviral transduction. DN3 cells were generated from lineage-negative Sc α 1⁺c-Kit⁺ precursors isolated from *Vav-Bcl2*-transgenic mice, infected with retrovirus encoding IRES-GFP or mouse c-Myc-IRES-GFP, sorted, placed in secondary cultures with OP9-DL1 cells and analyzed as described¹⁴.

Microarray hybridization and analysis. An Affymetrix MoGene 1.0 ST array was used for RNA processing and microarray analysis according to ImmGen standard operating procedures.

Bioinformatics analysis. Hierarchical clustering, principal-component analysis and Euclidian distance calculation were done on log₂-transformed mean-centered data sets filtered for expression values greater than 120 in any subsets and including only the 15% of probes with the highest variation across analyzed populations. Noisy probes (with an intra-population coefficient of variation (CV) of >0.65, or 0.35 < intra-population CV < 0.65 and interpopulation CV < 1 across the $\alpha\beta$ T cell ImmGen data set) were removed from all these analyses (463 probes were removed by these criteria, representing 1.8% of all probes). The Population PCA tool (<http://cbdm.hms.harvard.edu/LabMembersPages/SD.html>) was used for principal-component analysis. The HierarchicalClustering module from the GenePattern genomic analysis platform was used for hierarchical clustering, with Euclidian distance, and hierarchical clustering visualized with the HierarchicalClusteringViewer module of GenePattern. The Euclidian distance heat map was created with the HeatMapImage module of GenePattern. K-means clustering was done on a data set that included LT-HSC, ST-HSC, MPP, ETP, ETP-DN2a, DN2a, DN2b, DN3a, DN3b, DN3b-DN4, ISP, DP blast and small DP populations with the ExpressCluster 1.3 tool (<http://cbdm.hms.harvard.edu/LabMembersPages/SD.html>). Prefiltering on the probes that had expression values greater than 120 in at least one subset and changed their expression fourfold or more-between any of the populations was applied, resulting in the 2088 probes included in the analysis. Expression values were log₂-transformed and mean-centered. Euclidian distances were used as the distance metric. Probes within the resulting clusters were clustered with the HierarchicalClustering module for GenePattern with Euclidian distance as row distance and visualized with the HierarchicalClusteringImage module. The list of 2252 proliferation-related probes ('proliferation signature') was generated by merging of lists of all probes in the gene-ontology categories GO:0007049 (cell cycle), GO:0006259 (DNA metabolic process), GO:0005813 (centrosome), GO:0005819 (spindle) and GO:0000776 (kinetochore), as well as probes that detect histones. The 'Proliferation' index was calculated by averaging of row maximum normalized expression values for each probe in the proliferation signature. Likewise, the 'translation' index was calculated by averaging of row maximum normalized expression values for each probe in the gene-ontology categories GO:0006412 (translation) and GO:0005840 (ribosome). The DAVID bioinformatics database (Database for Annotation, Visualization and Integrated Discovery)^{88,89} and GOrilla gene-ontology enrichment analysis and visualization tool^{90,91} were used for analysis of gene-ontology categories enrichment. TCR

signaling-related genes from K-means clusters were mapped to the KEGG (Kyoto encyclopedia of genes and genomes) pathway^{92,93} with the Functional Annotation tool of DAVID^{88,89}.

Analysis of phosphorylation events by mass cytometry. Cells were stained according to published procedures⁸⁷. Fixed cells were incubated for 45 min at room temperature with a mixture of antibodies to surface markers (identified above) =, then were washed and permeabilized in methanol for 20 min at 4 °C. After the methanol was washed off, cells were stained for 45 min at room temperature with a mixture of antibodies to intracellular antigens (identified above), then were washed and then incubated for 20 min at room temperature in intercalator solution (paraformaldehyde 1.6% in 1× PBS), and then washed three times in double-distilled H₂O before multidimensional mass cytometry on a CyTOF (DVS) as described⁸⁷. Post-background subtraction and normalization Cytobank was used for analysis of data obtained by multidimensional mass cytometry.

86. Bouillet, P. *et al.* Proapoptotic Bcl-2 relative Bim required for certain apoptotic responses, leukocyte homeostasis, and to preclude autoimmunity. *Science* **286**, 1735–1738 (1999).
87. Bendall, S.C. *et al.* Single-cell mass cytometry of differential immune and drug responses across a human hematopoietic continuum. *Science* **332**, 687–696 (2011).
88. Huang, W., Sherman, B.T. & Lempicki, R.A. Systematic and integrative analysis of large gene lists using DAVID bioinformatics resources. *Nat. Protoc.* **4**, 44–57 (2009).
89. Huang, W., Sherman, B.T. & Lempicki, R.A. Bioinformatics enrichment tools: paths toward the comprehensive functional analysis of large gene lists. *Nucleic Acids Res.* **37**, 1–13 (2009).
90. Eden, E., Lipson, D., Yorgev, S. & Yakhini, Z. Discovering motifs in ranked lists of DNA sequences. *PLoS Comput. Biol.* **3**, e39 (2007).
91. Eden, E. *et al.* GOrilla: a tool for discovery and visualization of enriched GO terms in ranked gene lists. *BMC Bioinformatics* **10**, 48 (2009).
92. Kanehisa, M. & Goto, S. KEGG: Kyoto encyclopedia of genes and genomes. *Nucleic Acids Res.* **28**, 27–30 (2000).
93. Kanehisa, M. *et al.* KEGG for integration and interpretation of large-scale molecular data sets. *Nucleic Acids Res.* **40**, D109–D114 (2012).

Corrigendum: The transcriptional landscape of $\alpha\beta$ T cell differentiation

Michael Mingueneau, Taras Kreslavsky, Daniel Gray, Tracy Heng, Richard Cruse, Jeffrey Ericson, Sean Bendall, Matt Spitzer, Garry Nolan, Koichi Kobayashi, Harald von Boehmer, Diane Mathis, Christophe Benoist & the Immunological Genome Consortium
Nat. Immunol.; doi:10.1038/ni.2590; corrected online 13 May 2013

In the version of this article initially published online, the eighth and ninth author names were incorrect. Those should be Matthew H. Spitzer and Garry P. Nolan. The error has been corrected for the print, PDF and HTML versions of this article.